

SCRUTINIZATION OF FLOW CHARACTERISTICS THROUGH
ORIFICES

A THESIS SUBMITTED TO
THE GRADUATE SCHOOL OF NATURAL AND APPLIED SCIENCES
OF
MIDDLE EAST TECHNICAL UNIVERSITY

BY

TUĞÇE YILDIRIM

IN PARTIAL FULFILLMENT OF THE REQUIREMENTS
FOR
THE DEGREE OF MASTER OF SCIENCE
IN
CIVIL ENGINEERING

SEPTEMBER 2010

Approval of the thesis:

SCRUTINIZATION OF FLOW CHARACTERISTICS THROUGH ORIFICES
submitted by **TUĞÇE YILDIRIM** in partial fulfillment of the requirements
for the degree of **Master of Science in Civil Engineering Department,**
Middle East Technical University by,

Prof. Dr. Canan Özgen
Dean, Graduate School of **Natural and Applied Sciences**

Prof. Dr. Güney Özcebe
Head of Department, **Dept. of Civil Engineering**

Asst. Prof. Dr. Şahnaz Tiğrek
Supervisor, **Dept. of Civil Engineering, METU**

Examining Committee Members:

Prof. Dr. Melih Yanmaz
Civil Engineering Dept., METU

Asst. Prof. Dr. Şahnaz Tiğrek
Civil Engineering Dept., METU

Assoc. Prof. Dr. Ayşe Burcu Altan Sakarya
Civil Engineering Dept., METU

Asst. Prof. Dr. Mete Köken
Civil Engineering Dept., METU

Asst. Prof. Dr. Dilek Funda Kurtuluş
Aerospace Engineering Dept., METU

Date: 17/09/2010

I hereby declare that all information in this document has been obtained and presented in accordance with academic rules and ethical conduct. I also declare that, as required by these rules and ethical conduct, I have fully cited and referenced all material and results that are not original to this work.

Name, Last name: Tuğçe Yıldırım

Signature:

ABSTRACT

SCRUTINIZATION OF FLOW CHARACTERISTICS THROUGH ORIFICES

Yıldırım, Tuğçe

M.Sc., Department of Civil Engineering

Supervisor: Asst. Prof. Dr. Şahnaz Tiğrek

September 2010, 61 pages

Orifices are essential devices for measurement and control of flow. It is important to define the flow field and understand the flow characteristics behind an orifice for the sake of reliability measures in many hydraulic engineering applications. Since analytical and experimental solutions are restricted, a numerical solution is obtained using volume of fluid (VOF) method with the CFD solver, FLUENT, for sharp crested orifices, orifice tubes and slots. The results are compared to the available data in the literature; also a large spectrum of data collection has been achieved.

Keywords: orifice flow, orifice tube, coefficient of discharge, volume of fluid, flow measurement.

ÖZ

ORİFİS AKIM KARAKTERİSTİKLERİNİN İRDELENMESİ

Yıldırım, Tuğçe

Yüksek Lisans, İnşaat Mühendisliği Bölümü

Tez Yöneticisi: Yrd. Doç. Dr. Şahnaz Tiğrek

Eylül 2010, 61 sayfa

Orifisler, debi ölçümü ve akım kontrolü için önemli yapılardır. Hidrolik mühendisliği uygulamalarının güvenilirliğini sağlamak adına orifislerin arkalarında oluşan akım alanının tanımlanması ve akım karakteristiklerinin belirlenmesi önem arz etmektedir. Analitik ve deneysel çözümlerin sınırlı olması dolayısıyla keskin kenarlı orifisler, tüp orifisler ve yarıklar için sayısal model ve inceleme akışkan hacmi yöntemi ile FLUENT'i kullanarak yapıldı. Sonuçların karşılaştırılması ve doğrulanması için literatürdeki deneysel veriler kullanılırken, bu alanda geniş bir veri yelpazesi de elde edildi.

Anahtar kelimeler: Orifis akımı, orifis tüp, boşaltma katsayısı, akışkan hacmi yöntemi, debi ölçümü.

To my family & friends

ACKNOWLEDGMENTS

First of all, I would like express my sincere gratitude to Asst. Prof. Dr. Şahnaz Tiğrek, for her support, patience, encouragement and confidence on me in every stage of this study.

Secondary, I would like to thank you Mr. Onur Dündar. I am grateful of his support and effort during this study.

Then, my heartiest thanks go to Nazlı Aslıcan Yılmaz, for showing me every kind of help and support at every turn.

I want to show my appreciation to Meriç Apaydın, Gizem Okyay and Ezgi Köker for their companion.

My deepest gratitude goes to my parents for their endless support during this study as in the entire of my lifetime.

Founding of the FLUENT software used within the scope of the study was provided by State Planning Organization via the project: *Experimental and Numerical Investigation of Dam Siltation and Discharging of the Sediment entered into Dam reservoir to the Downstream*. BAP-03-03-DPT.2003(06)K120920-23. The authors acknowledge invaluable support of State Planning Organization of Turkey.

TABLE OF CONTENTS

ABSTRACT	iv
ÖZ.....	v
ACKNOWLEDGMENTS.....	vii
TABLE OF CONTENTS	viii
LIST OF TABLES.....	x
LIST OF FIGURES.....	xi
LIST OF SYMBOLS.....	xiii
CHAPTERS	
1. INTRODUCTION.....	1
1.1. Introduction and The Scope of The Study	1
2. THEORETICAL BACKGROUND.....	3
2.1. General Information.....	3
2.2. Methodology	6
2.3. Review of The Discharge Correction Coefficients	10
2.3.1. Sharp Crested Orifices.....	11
2.3.2. Orifice Tubes	15
3. FLUENT AS A TOOL FOR NUMERICAL SOLUTION	20
3.1. General Information.....	20

3.2. Modeling of The Problem and Boundary Conditions.....	21
3.3. Volume of Fluid Method.....	23
3.4. The 2-D Simulation of The Slots	25
4. FLOW SCRUTINIZATION.....	32
4.1. General Information.....	32
4.2. Physical Model.....	32
4.2.1. Sharp Crested Orifices.....	34
4.2.2. Circular Tube Orifices.....	39
4.3. Post Processing of The Solutions.....	45
4.3.1. Sharp Crested Orifices.....	45
4.3.2. Circular Tube Orifices.....	48
5. CONCLUSION	55
REFERENCES.....	57

LIST OF TABLES

TABLES

Table 2.1: Parameters used in the dimensional analysis of C_d	8
Table 4.1: A summary of all the runs.....	44

LIST OF FIGURES

FIGURES

Figure 2.1: Orifice a) sharp crested b) on a wall with a thickness	5
Figure 2.2: Tube Orifice a)short b) long	5
Figure 2.3: Discharge coefficient curve according to Lea and Merritt.....	13
Figure 2.4: Theoretical and experimental discharge coefficients	14
Figure 2.5: Discharge coefficients (Çobanoğlu, 2008)	17
Figure 2.6: Discharge coefficients for orifice tubes (Simon, 1981).....	19
Figure 3.1: Geometrical properties of slots represented in 2-D	26
Figure 3.2: Coarse mesh for 2-D slot model	28
Figure 3.3: Fine mesh for 2-D slot model	28
Figure 3.4: Velocity contours.....	29
Figure 3.5: The total pressure contours	30
Figure 3.6: Pathlines inside of the reservoir	31
Figure 3.7: Velocity vectors close to the outlet.....	31
Figure 4.1: Front view of the setup of Çobanoğlu (2008).....	34
Figure 4.2: Fine mesh for sharp crested orifice.....	36
Figure 4.3: Coarse mesh for sharp crested orifice.....	36
Figure 4.4: Boundary types of the model.....	37

Figure 4.5 Comparison of centerline velocity profile for sharp crested orifice inviscid flow solution with fine mesh	38
Figure 4.6: Comparison of centerline velocity profile for sharp crested orifice inviscid flow solution with coarse mesh	38
Figure 4.7: Comparison of centerline velocity profile for sharp orifice turbulent flow solution with coarse mesh.....	39
Figure 4.8: General view of the tank model	40
Figure 4.9: Boundary conditions for orifice tube	41
Figure 4.10: Re versus C_d graph for various data and cases	42
Figure 4.11: Velocity contours of Case 1A	46
Figure 4.12: Total pressure contours of Case 1A	46
Figure 4.13: Contours of velocity of Case 1A side	47
Figure 4.14: Velocity contours of the outlet for Case 3B.....	48
Figure 4.15: Velocity contours of the outlet with grid for Case 3B	49
Figure 4.16: Velocity contours for the centerline of the tube for Case 3B...	49
Figure 4.17: Mass flow rate versus. iteration on outlet for Case 3B	50
Figure 4.18: Residuals for Case 3B	51
Figure 4.19: Contours of total pressure on outlet for Case 3B.....	51
Figure 4.20: Contours of total pressure for Case 3B.....	52
Figure 4.21: Contours of total pressure on the tube for Case 3B.....	53
Figure 4.22: Velocity vectors in the tube for Case 3B	53
Figure 4.23: Velocity vectors for every 5 mm of tube for Case 3B	54

LIST OF SYMBOLS

A	: Area
C_c	: Coefficient of contraction
C_d	: Discharge coefficient
C_v	: Coefficient of velocity
e	: Entrance shape
h	: Head over orifice
d	: Diameter of the orifice
f	: Friction factor
g	: Gravitational acceleration
l	: Orifice tube length
l_e	: Entrance length
k_r	: Roughness
k	: Turbulent kinetic energy
\dot{M}	: Mass flux
p	: Pressure
Re	: Reynolds number
Q	: Discharge
U_o	: Uniform velocity
v	: Ideal velocity
V	: Average velocity
V_c	: Centerline velocity
w_r	: Width of the tank
α	: Energy correction coefficient
β	: Momentum correction coefficient
ρ	: Density
ν	: Kinematic viscosity
μ	: Dynamic viscosity
γ	: Specific weight
σ	: Surface tension coefficient
CFD	: C omputational F luid D ynamics
VOF	: V olume o f F luid
PIV	: P article I mage V elocimeter
PRESTO	: P ressure S taggering O ption

CHAPTER 1

INTRODUCTION

1.1 INTRODUCTION AND THE SCOPE OF THE STUDY

A simple orifice finds a large area of application as a measurement structure and/or a control structure. They can be addressed as an intake if they are installed to a storage reservoir of a water supply. Although there are several studies about calibration of the orifices, there are very limited studies that analyze the flow in front of and/or through the orifices. Nevertheless, understanding of an orifice flow is an important way to determine the losses and consequently to make measurements accurately.

In hydraulic engineering applications, namely fish entrainment studies, flow in the sedimentation tanks, flow induced by the sluice gates, selective withdrawal from a reservoir and analysis of the flow at the upstream of an intake are important concepts (Gerges and McCorquodale, 1997; Shammaa and Zhu, 2010). In the design of a fish repulsion system the acceleration zone behind the intake should be identified (Islam and Zhu, 2010). The proper screen placement should be chosen so the fish will not be stuck on the high velocity zone (Shammaa et al., 2005). Also the movement of sediment behind the orifices gains significance when they are placed in

reservoirs and ponds and it can be predicted with the understanding of flow behind orifices (Göbelez, 2008).

There are few studies in the literature to examine the flow in front of an intake structure. So far the potential flow theory was used to describe the flow field. However, the potential flow theory can describe the flow field behind an intake properly within a distance up to three times of the orifice diameter from the intake but; beyond this range development of a jet and stratification cause the deviation of the flow field from the theory (Shammaa and Zhu, 2010).

Therefore, the scope of this study is to understand the flow field by means of velocity profiles, coefficient of discharge, pressures and streamlines etc. with the help of commercial software FLUENT.

In the way to achieve these targets, the historical background of this topic which extend over a hundred years is reviewed and compiled within the present study.

Therefore in Chapter 1 a very brief description of the problem is given. There is a very detailed literature review in Chapter 2. Chapter 3 is reserved to introduce FLUENT software within the concept of the study. Chapter 4 presents the numerical model and its results. Finally, Chapter 5 comprises the conclusions.

CHAPTER 2

THEORETICAL BACKGROUND

2.1 GENERAL INFORMATION

Reservoirs or tanks can be controlled by number of hydraulic structures, such as sluice gates, weirs, pipes and orifices. These types of structures may be classified into two groups. In one group, the flow takes place under pressure through a fixed cross section as is the case for orifices, nozzles, short tubes, sluiceways and gates. The second group includes cases in which the flow occurs through an initially undetermined cross section, such as over weirs, spillways, chutes and drop structures (Simon, 1981).

An orifice used to measure the flow rate out of a reservoir or through a pipe is an opening on a wall of a tank or in a plate normal to the axis of a pressurized pipe. The opening that the fluid flows through is usually circular, although it may have a square-edged or rounded entrance. An orifice can be placed in the side walls or at the bottom of a reservoir or tank. The orifice is called an orifice plate or orifice meter if it is installed on a plate at the end of the pipe or some other intermediate location (Streeter, 1966; Daugherty and Franzini, 1977 and Douglas et al., 2001). A standard orifice as depicted in Fig. 2.1a is characterized by the thickness of the wall

or plate being very small relative to the size of the opening, and it also has a sharp edge or absolutely square shoulders (Daugherty and Franzini, 1977). If the plate is thick as in Fig. 2.1b, then it is referred to as an orifice tube (Daugherty and Franzini, 1977). Often, the case that structural requirements necessitate a thick wall. Thus, flow conditions through the orifice are affected by the plate thickness, surface roughness and the radius of curvature. In addition, there can be an extension that is 2- to 3-times the orifice diameter that delivers the fluid away from the storage structure. In this case, the flow is also affected by the pipe characteristics. These types of orifices (Fig. 2.2a) are known as short tube orifices (Brater and King, 1982). It is also possible to increase the extension to deliver fluid to a distance, so that the length extends beyond 2-to 3-times the orifice diameter; these are classified as long tube orifices (see Fig. 2.2b). There is no clear distinction between tube and thick walled orifices (Daugherty and Franzini, 1977). The term orifice tube can denote an orifice having considerably thickness or an extension from the structure. For clarity, orifice tubes installed in a pipe will be referred to as orifice tubes throughout this study.

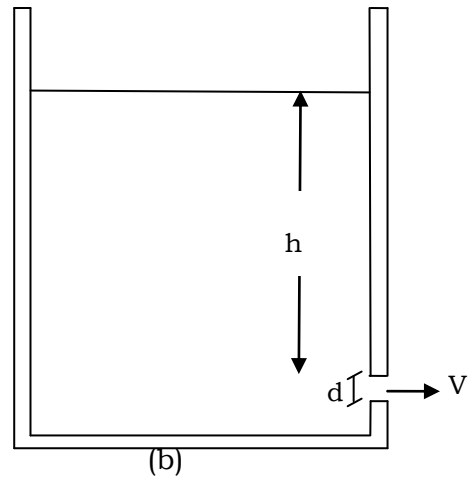
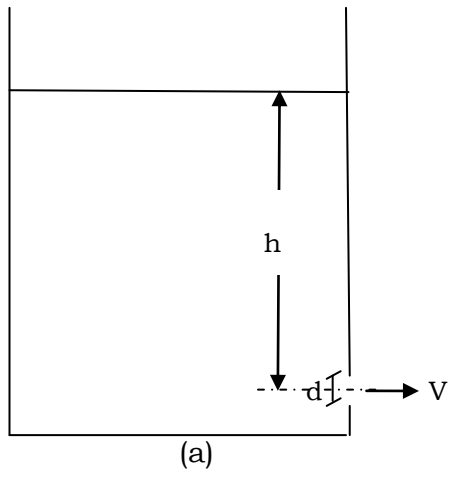


Figure 2.1: Orifice a) sharp crested

b) on a wall with a thickness

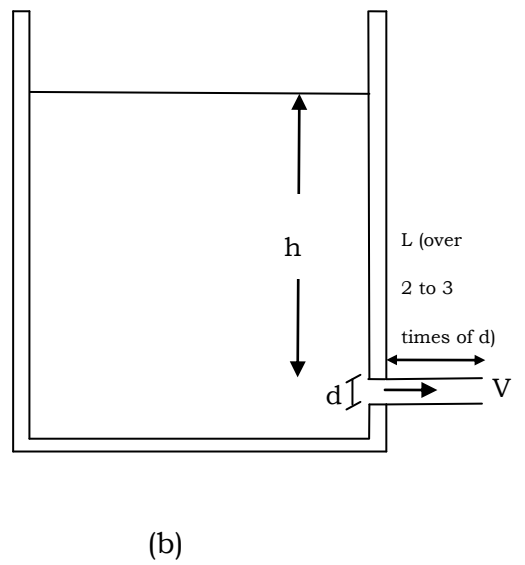
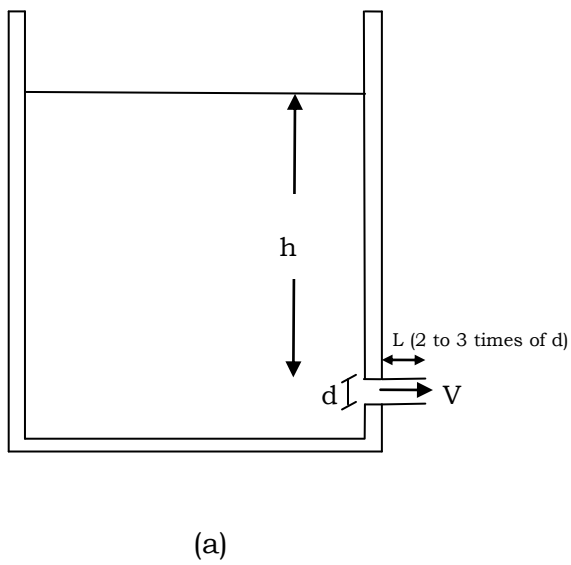


Figure 2.2: Tube Orifice a) short

b) long

2.2 METHODOLOGY

The amount of fluid discharged from a reservoir through an opening can be quantified via a calibration process. In this case there will be a jet streaming from an orifice. The jet is considered to be submerged if it is surrounded by a fluid (Brater and King, 1982). The streamlines converge near the outlet. They converge further beyond the outlet until the streamlines become parallel with each other. This section has the minimum jet cross sectional area and is denoted the *vena contracta*. Beyond the *vena contracta*, the streamlines diverge due to the frictional effect of the horizontal jet and converge in the vertical jets. The potential energy of the upstream still water is converted into the kinetic energy of the free jet through the openings. Neglecting losses, the Bernoulli equation can be used to represent the energy balance for this situation. If the Bernoulli equation is written between water surface (denoted subscribed 1) and jet centerline by taking the reference as orifice/orifice tube centerline(denoted subscribe 2), the following expression will be obtained:

$$\frac{v_1^2}{2g} + \frac{p_1}{\gamma} + h = \frac{v_2^2}{2g} + \frac{p_2}{\gamma} \quad (2.1)$$

where v_1 is the velocity at the water surface

v_2 is the velocity at the jet

p_1 is the pressure at the water surface

and p_2 is the pressure at the jet centerline

If it is assumed that the velocity at the outlet jet is uniformly distributed, then the pressure can be accepted to be atmospheric pressure at the cross section, Eqn. 2.1 will be reduced into following equation,

$$h = \frac{v_2^2}{2g} \quad (2.2)$$

$$v_2 = \sqrt{2gh} \quad (2.3)$$

However, in reality, the fluid is viscous, and no-slip boundary conditions prevail. Therefore, a velocity profile occurs at the outlet. The observed discharge will be a product of the cross sectional average velocity, V , and the outlet area, A . If the relationship between ideal velocity, v_2 and observed velocity is described as $V = C_d v_2$, then the observed discharge is described as follows:

$$Q = V \times A = C_d \times A \times v_2 = C_d \times A \times \sqrt{2gh} \quad (2.4)$$

The discharge coefficient, C_d , includes the coefficient of contraction, C_c , and the coefficient of velocity, C_v ;

$$C_d = C_c \times C_v \quad (2.5)$$

The discharge coefficient, C_d , of an orifice or an orifice tube are generally defined as a function of orifice geometry, fluid properties and flow characteristics, which are presented in Table 2.1.

Table 2.1: Parameters used in the dimensional analysis of C_d

Components	Symbol	Physical Quantity	Dimension
Tank	w_r	Width of the tank	L
Properties of short tube orifice	d	Orifice diameter	L
	ℓ	Orifice length	L
	k_r	Roughness of the pipe	L
	e	Entrance shape	-
Flow Characteristics	Q	Discharge	L^3T^{-1}
	g	Gravitational acceleration	LT^{-2}
Fluid Characteristics	ρ	Density of the fluid	ML^{-3}
	μ	Dynamic viscosity	$ML^{-1}T^{-1}$
	σ	Surface tension	MT^{-2}

The functional relationship of these parameters can be written as:

$$C_d = f_1(w_r, d, \ell, k_r, e, Q, g, \rho, \mu, \sigma) \quad (2.6)$$

By choosing d , Q and ρ as repeating variables, the functional relationship in dimensionless terms is:

$$C_d = f_2\left(\frac{w_r}{d}, \frac{\ell}{d}, \frac{k_r}{d}, e, \frac{gd^5}{Q^2}, \frac{d\mu}{Q\rho}, \frac{d^3\sigma}{\rho Q^2}\right) \quad (2.7)$$

In Eq. (4), the 5th term on RHS (gd^5/Q^2) is $(16/\pi^2 Fr^2)$, where Fr is the Froude number, and the 6th term ($d\mu/Q\rho$) on RHS is $(4/\pi Re)$, where Re is the Reynolds number defined as

$$Re = Vd\rho/\mu \quad (2.8)$$

The 7th term on RHS is the Weber number. The influence of the all terms will not be observed in each specific case such as,

i) If the orifice is small compared to the tank, the reservoir width will not be an effective parameter. An orifice is defined as small if the orifice head is greater than five times the height of the orifice opening (Gupta, 1989).

ii) If there were no air entrainment and vortex formation; the Froude Number can be ignored. Bos (1989) stated that for true orifice flow to occur, the upstream water level must always be well above the top of the opening, such that vortex flow with air entrainment is not evident.

ii) Finally, the Weber number effect will be negligible for high flow rates (Lienhard V and Lienhard IV, 1984 and Aydın et al., 2006).

2.3 REVIEW OF DISCHARGE CORRECTION COEFFICIENTS

Understanding and predicting the relationship between pressure drop or head loss and flow rate through orifices is essential for the design and evaluation of fluid power and control devices, (Simon 1981 and Jankowski et al., 2008). Although this relationship is well understood for sharp crested orifices at high Reynolds numbers for Newtonian fluids, many recent studies have attempted to characterize and explain the observed pressure drop for flow through pipe micro-orifices (Jankowski et al., 2008), which have large length-to-diameter ratios. Small orifice configurations are widely used in micro-scale thermal and mechanical systems (Tu et al., 2006) and are important in understanding the behaviour of a number of biofluid systems involving the drainage of fluids through capillaries (Phares et al., 2005). Additionally, flow through periodically arranged micro-scale orifice tubes has been suggested as a model for flow through porous media (Liu et al., 2001). Orifice calibration for non-Newtonian fluids is under investigation due to process industry needs, (Dziubinski and Marcinkowski, 2006). Furthermore, the simplicity of short tubes is making them very popular for residential uses, (Yang and Zhang 2005 and Costola and Etheridge, 2008).

There is limited research on short tube orifices. Davis (1952) reported discharge coefficients for large orifices and tubes. He introduced orifice geometry as a parameter that influences flow. Dally et al. (1993) reported some findings on short tube orifice discharge coefficients. Dziubinski and Marcinkowski (2006) studied the discharge of Newtonian and Non-Newtonian liquids from tanks through short tube orifices and reported findings on discharge coefficients.

2.3.1 SHARP CRESTED ORIFICES

One of the earliest researchers who gave discharge coefficients for a large range of Reynolds number was Lea (1938 and 1942) (cited in p. 4-8 of Brater and King, 1982 and Swamnee and Swamnee, 2010). Lea conducted more than 100 experiments with several working fluids of water, mixtures of water and glycerin and a number of oils. Brater and King (1982) gave a curve in which discharge coefficient values were plotted against the Reynolds number. In the present study, Lea's curve reproduced from the graph given in the study of Swamnee and Swamnee, (2010) by reading points by commercial software FINDGRAPH. This curve is given in Fig. 2.3. One should note that there are some discrepancies between two curves given by Brater and King and Swamnee and Swamnee. However, it is preferred to use the latest one.

It is widely accepted that the flow is laminar up to Reynolds number value of 10 and is fully turbulent for Reynolds number greater than 10000. And intervening values are corresponding to a transient flow (Brater and King, 1982).

Further Merritt (1967) was theoretically formulated orifice discharge coefficients within a pressurized pipe. Fig. 2.3 shows reproduction of Merritt's curve, too. The resemblance of the two curves let us to derive following findings;

i) The laminar region may be accepted to vary linearly with the square root of the Reynolds number. Here, some of the important studies are summarized as follows:

- Sampson et al. (1891) (Cited in Jankowski et. al. 2008) and Dagan et. al. (1982):

$$C_d = 0.163\sqrt{Re} \quad (2.9)$$

- Merritt (1967)

$$C_d = 0.2\sqrt{Re} \quad (2.10)$$

- Kiljanski (1993)

$$C_d = 0.141\sqrt{Re} \quad (2.11)$$

- Dzubinski and Marcinkowski (2006)

$$C_d = 0.186\sqrt{Re} \quad (2.12)$$

ii) There is an overshooting in transition region. However, there are limited number of experimental observations for this region (Dzubinski and Marcinkowski, 2006, and Çobanoğlu, 2008)

ii) There is a tendency of constant iterative Cd values of 0.61 in the fully turbulent region. There are several studies support this argument (Smith, 1886; Bovey, 1909 and Fanning 1906 cited in Brater and King, 1982 on p. 4-6; Judd and King (1908) cited in Lienhard V and Lienhard IV, 1984 and Dally, et al., 1993)

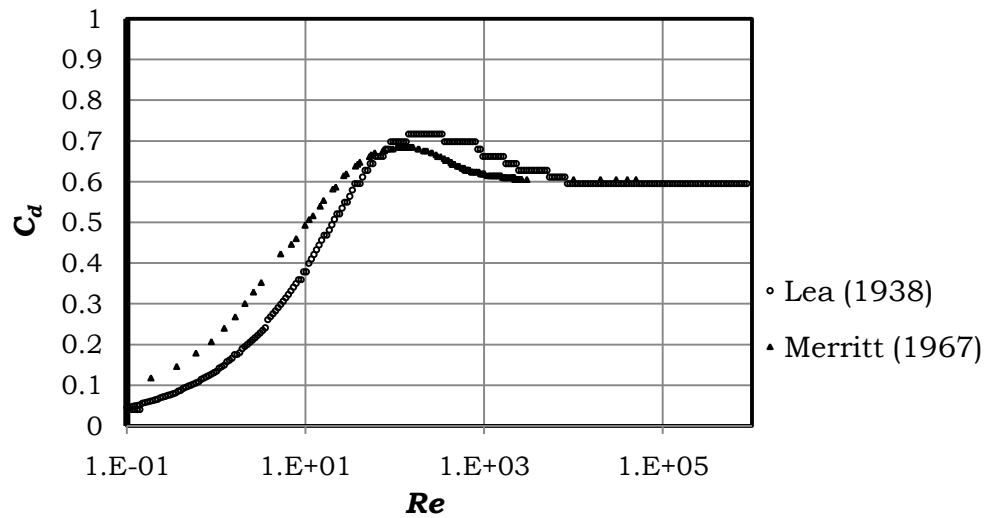


Figure 2.3: Discharge coefficient curve according to Lea and Merritt.

Recently, Swamee and Swamee (2010) proposed the following equation which is the formulated form of Lea's curve:

$$C_d = 0.611 \left[87 \left(\frac{v}{d\sqrt{gh}} \right)^{1.43} + \left(1 + \frac{4.5v}{d\sqrt{gh}} \right)^{-1.26} \right]^{-0.7} \quad (2.13)$$

Figure 2.4 compares all those theoretical equations and some data collected from literature with Lea's curve.

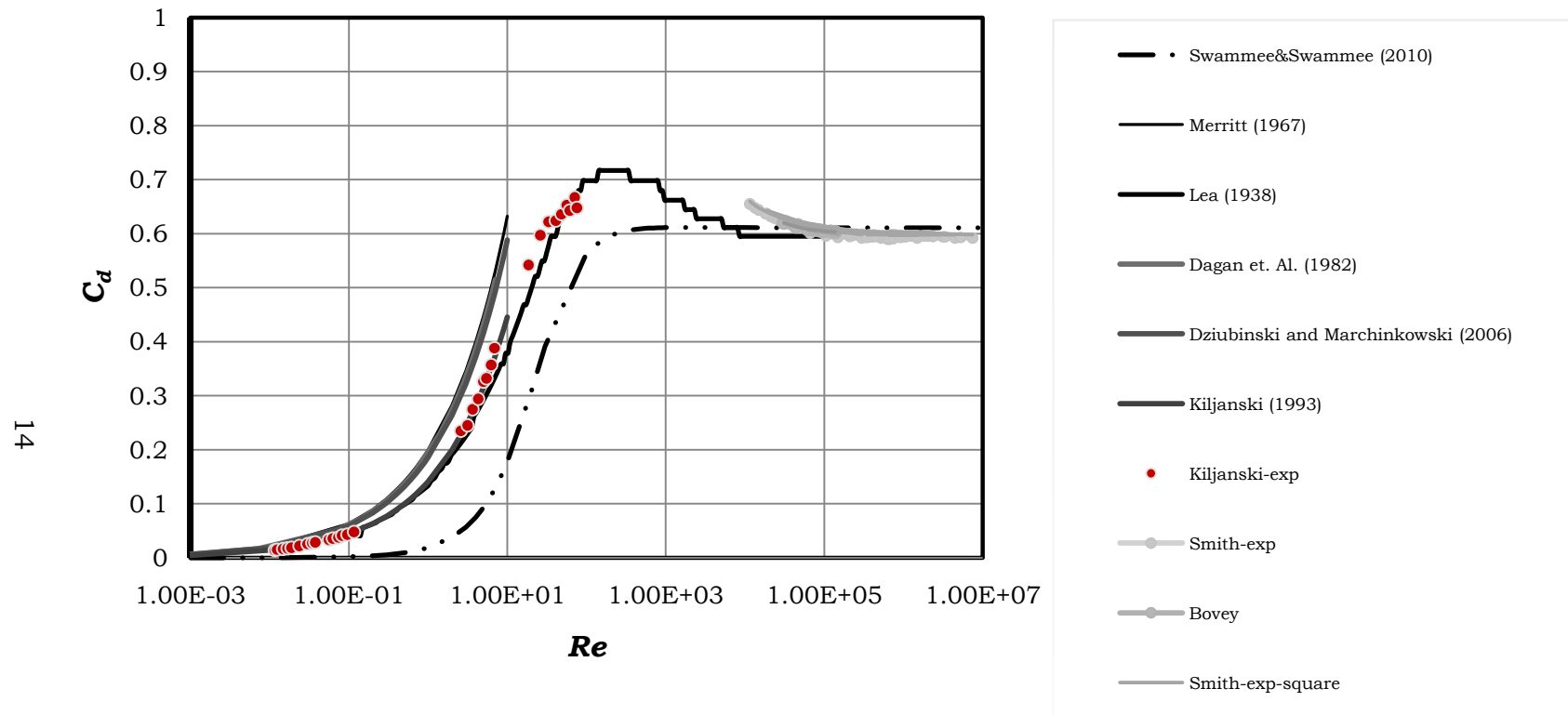


Figure 2.4: Theoretical and experimental discharge coefficients

2.3.2 ORIFICE TUBES

Discharge coefficient values are observed for several length and entrance shape of the orifice by Davis (Davis, 1952). He classified tube orifices according to their length and entrance type. Length varied from 0.31 ft (0.09 m) to 14 ft (4.27 m). The tube entrance varied from sharp crested to 4-sided elliptical. Davis (1952) reported the discharge coefficient, C_d ranging from 0.62 to 0.96, for several combinations of entrances and lengths. On the other hand, Dally et al. (1993) also recommended C_d values for both submerged and free jets. In their study, C_d has a value of 0.8 for short tubes. They also suggest a value of 1.00 for C_c and a value of 0.80 for C_v in case of a short tube. However, the reported values are limited to $\ell/d = 2.5$.

The ratio of the length to the diameter of an orifice, ℓ/d , is a significant parameter that affects the performance of a tube orifice in terms of frictional losses through the tube.

Kiljanski (1993) carried out a series of experiments to examine the performance of orifices for Newtonian and Non-Newtonian liquids discharging from tanks, and proposed the following equations:

$$C_d = 0.124\sqrt{Re} \quad \text{for } \ell/d = 0.5 \quad (2.14a)$$

$$C_d = 0.1982\sqrt{Re} \quad \text{for } \ell/d = 1.0 \quad (2.14b)$$

The discharge coefficient is directly proportional to the square root of Reynolds number for $Re < 10$, which is in the laminar flow regime.

Dziubinski and Marcinkowski (2006) used several orifice diameters in their experiments with changing lengths. The orifice diameters were 5, 8, 12.5 and 17 mm. Length-to-diameter ratios were 0, 0.35, 0.5, 0.75, 1 and 3. Data were

collected for Newtonian and Non-Newtonian fluids with various viscosities like water, ethylene glycol and water solutions of starch syrup. They gave the relationship between discharge coefficient, C_d and Reynolds number, Re for their experiments.

$$C_d = \left[0.186 - 0.0756 \left(\frac{\ell}{d} \right)^{0.333} \right] \sqrt{Re} \quad (2.15)$$

In the study of Çobanoğlu (2008), the performance of freely discharging orifice tubes under constant head was investigated. Tubes having two different diameters (6.00 and 10.35 mm) and two length-to-diameter ratios (5 and 8) were tested, (see Fig. 2.5). For the range of the Reynolds numbers examined ($2300 < Re < 18600$), the discharge coefficient, C_d varies with both the Reynolds number and the length-to-diameter ratio. The location and magnitude of the peak was reported to be a function of Re and ℓ/d . However, since the range of Reynolds number fell into transient flow region, any formulation could not be obtained.

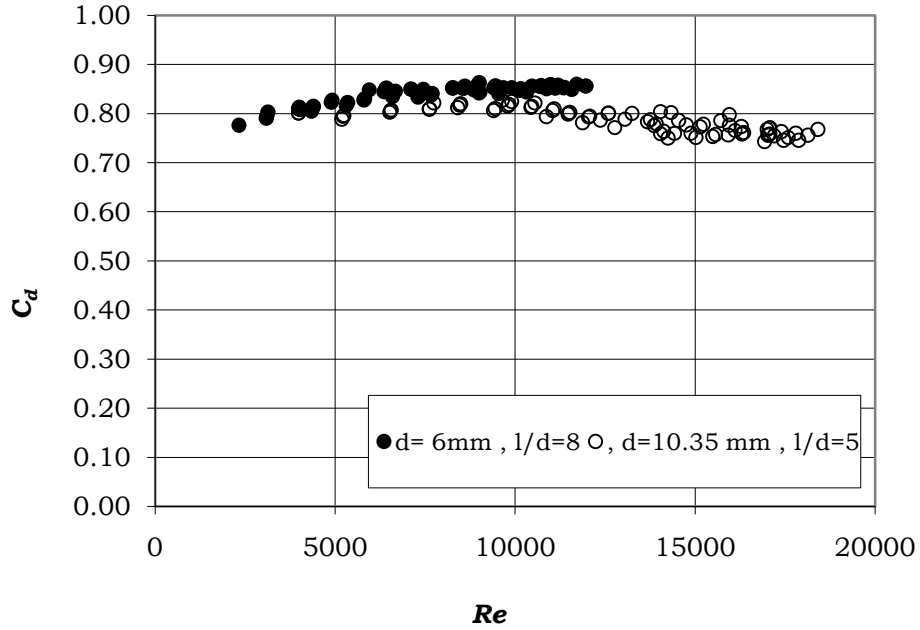


Figure 2.5: Discharge coefficients (Çobanoğlu, 2008)

There are several studies in which the discharge coefficient in orifice tubes were tried to be formulated analytically (Borutzky et al., 2002 and Jankowski et al., 2010). The basic idea in the study of Jankowski et al. is to formulate the discharge coefficients as a sum of frictional losses and entrance losses of sharp crested orifices. However, the comparison of the results with experimental data is not promising and they are overestimating. The reasons can be counted as follows:

- i) Jankowski et al. (2010) did not consider possible reduction of the discharge coefficient of sharp crested orifice due to suppress contraction. Thus, when flow enters into the tube, there may not be separation and consequently vena contracta.

ii) They did not consider additional pressure drop within the tube due to boundary layer development. Tigrék (1990) was formulated pressure drop, Δp , at the entrance of a pipe as follows:

$$\frac{\Delta p}{\gamma} = \frac{V^2}{2g} \left(f \frac{\ell_e}{d} + 2(\alpha - \beta) \right) \quad (2.16)$$

in which ℓ_e is the length of the entrance where the velocity profile develops from uniform flow to the fully developed flow; α and β are the energy and momentum correction coefficients, respectively. The second term represents the additional losses due to developing flow. If the tube is extended further than the entrance region frictional losses will dominate. Thus, losses will increase as the length of the tube increase for high Reynolds number flows. Simon (1981) proposed the Figure 2.6 as a design chart. Although, there is no information about the Reynolds number range, it is assumed to be for high Reynolds numbers. This figure shows that, as the length of the tube increases the discharge coefficient value decreases, thus losses are increasing.

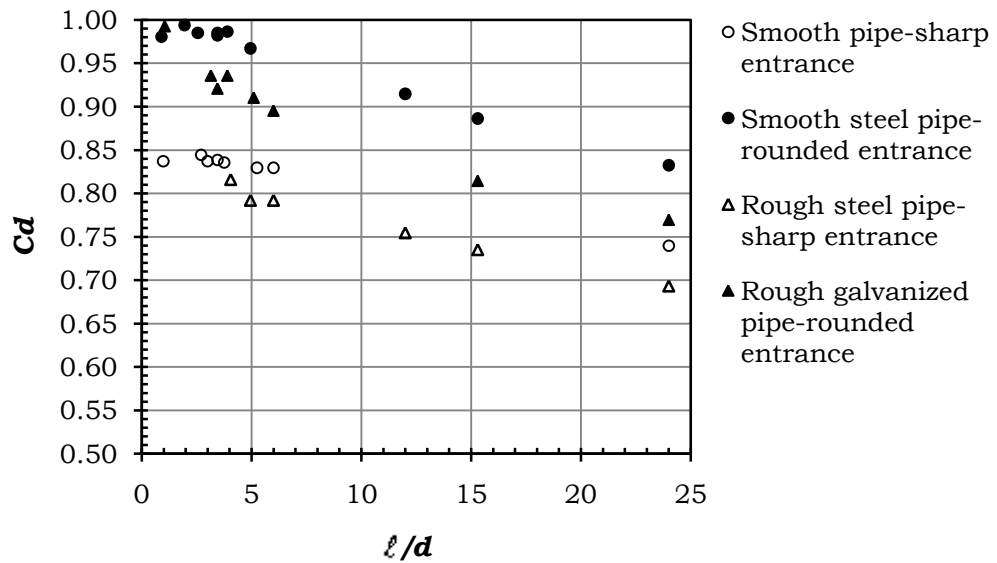


Figure 2.6: Discharge coefficients for orifice tubes (Simon, 1981)

It is quite difficult to collect data in a wide range of Reynolds number with one setup in the laboratory. Therefore, in this thesis it is preferred to construct a numerical model to scrutinize the flow around both a sharp crested orifice and a tube orifice in order to understand the flow behavior in the transient region. It should be noted that there may be different types of flow within the tank from which orifices protrudes within the orifice tube.

CHAPTER 3

FLUENT AS A TOOL FOR NUMERICAL SOLUTION

3.1 GENERAL INFORMATION

The scrutinization of the flow at the upstream of an orifice and flow through the orifice has been carried by the software FLUENT version 6.3.26 (ANSYS, 2010). FLUENT is a computational fluid dynamics program using control volume approach. Since 1983, it has a worldwide usage in different branches of the industry and it has been developing day by day to be the most used program in the field of Computational Fluid Dynamics (CFD).

FLUENT has a general computational fluid dynamics program in order to calculate fluid mechanics and heat transfer problems and belongs to a wide range of area such as automobile, aeronautical, chemical, food, household appliances and turbo machines industries (fan, compressors, pumps, turbines etc.). FLUENT used in the design of an unmanned underwater device, (Cevheri, 2009) and in the simulation of turbulent jets (Peker, 2005). However, usage of it in civil engineering problems is not very common due to shortage of information in open channel flow applications, which is one of the important topics for civil engineers. However, it records some developments in the last

ten years. Since usage of FLUENT in hydraulic problems has been increasing all around the world, some conclusions can be obtained from a few successful examples.

FLUENT has an advanced solver technology and includes different physical models, it can be used in laminar, transition and turbulent flows, and together with transport, convection and radiation of the heat transfer modes. It is a computational flow dynamics solver for both compressible and incompressible fluids. It can bring effectiveness and sensitivity to the solution of a large number of flow regimes with a multiple mesh generation that accelerates convergence with multiple solver options.

Further, there is a great convenience due to its ability of stopping the calculations and continuing at any moment during the calculations.

3.2 MODELING OF THE PROBLEM AND BOUNDARY CONDITIONS

The geometry, mesh and grid required for the solution is prepared by the help of GAMBIT, pre-processor software of ANSYS, version 2.4.6. (ANSYS, 2010)

In order to simulate the flow, at first the physical model is built in GAMBIT program. Then it is meshed and the boundary types are specified. After that, the meshed structure is transferred to the FLUENT program.

Calculations can be made as the flow is inviscid, laminar or turbulent that assigned in the viscous model. It is the choice of the user to make appropriate selection. There are several turbulence models available. Among them, standard k - ϵ and realizable k - ϵ were used in this study.

Standard k - ϵ is based on two transport equation model solving for turbulent kinetic energy, k and dissipation rate of the turbulent kinetic energy, ϵ . This is

the default k - ϵ model. Coefficients are empirically derived, valid for fully turbulent flows. There are options to account for viscous effects if the Reynolds number is low (ANSYS, 2006).

Realizable k - ϵ is a variant of the standard k - ϵ model. Its 'realizability' stems from changes that allow certain mathematical constraints to be satisfied for ultimately improving the performance for the low Reynolds numbers (ANSYS, 2006).

Since the physical model consists of a tank and an opening/a tube, type of flow is mixed. Such as the flow within the tube is pressurized flow but the flow in the tank is open to atmosphere. Also there is another inlet attached to the tank simulating source of the fluid. Thus, as a boundary condition, mass inlet was applied to the inlet of the tank. Pressure outlet boundary condition is applied to the top of the tank and to the exit of the outlet. Smooth wall boundary conditions are applied to the solid domain.

Since, the flow is a mixed two- phase flow with fluids of air and water, namely Volume of Fluid (VOF) is used to simulate the problem.

Although the final state of the flow is a steady flow in this selected particular problem, unsteady form of the flow equations are used for the reason that flow is unsteady until a constant head is satisfied. Thus initial conditions of velocity field is taken as if that the flow within the tank is still.

Some constants are used, such as; Atmospheric pressure: 101325 Pa, Gravitational acceleration: 9.81 m/s². In addition, the density and the dynamic

viscosity of the water are taken as 998.2 kg/m³ and 0.001003 kg/m-s, respectively. The other working fluid is air and has a density and dynamic viscosity as 1.225 kg/m³ and 1.7894e-05 kg/m-s, respectively.

3.3 VOLUME OF FLUID METHOD

In the simulation the Volume of Fluid model (VOF) is used, with two immiscible fluids as air and water-liquid. The material properties of these phases are used as defined in the FLUENT database and given in Section 3.2. The air is assigned as the primary phase and the water is the second phase. The volume of fluid method is a free surface tracking technique applied to a fixed Eulerian mesh, which enables the computation of multiple phase flow under the condition that they will not mix (Hirt, 1981).

The VOF method evaluates the construction of interface within the computational domain. It solves a single set of momentum equations for all fluids (Eqn. 3.1) and tracking the volume fraction of each of the fluids throughout the domain. (FLUENT, 2005)

$$\frac{\partial}{\partial t}(\rho \vec{v}) + \nabla \cdot (\rho \vec{v} \vec{v}) = -\nabla p + \nabla \cdot [\mu(\nabla \vec{v} + \vec{v}^T)] + \rho \vec{g} + \vec{F} \quad (3.1)$$

where; F represents the volumetric forces at the interface resulting from the surface tension.

The capturing of the interface between n numbers of phases is obtained by the solution of a continuity equation (Eqn. 3.2) for the volume fraction of one of the phases.

$$\frac{1}{\rho_q} \left[\frac{\partial}{\partial t} (\alpha_q \rho_q) + \nabla \cdot (\alpha_q \rho_q \vec{v}_q) = \sum_{p=1}^n (\dot{m}_{pq} - \dot{m}_{qp}) \right] \quad (3.2)$$

where \dot{m}_{pq} is the mass transfer from phase q to phase p and \dot{m}_{qp} is the mass transfer from phase p to phase q and α_q is the q^{th} fluid's volume fraction and:

$\alpha_q = 0$: The cell is empty (of the q^{th} fluid)

$\alpha_q = 1$: The cell is full (of the q^{th} fluid)

$0 < \alpha_q < 1$: The cell contains the interface between the q^{th} fluid and one or more other fluids.

The volume fraction equation is not solved for the primary phase. The volume fraction of the primary phase is computed with the constraint that total volume of fraction in any cell should be equal to one as in equation 3.3. The volume fraction equation is solved through explicit time discretization. In the solution of momentum equation whole domain is solved like single phase, and the resulting velocity field is shared among the phases. The momentum equation is dependent on the volume fractions of all phases through the material properties, density ρ and dynamic viscosity μ of each fluid.

$$\sum_{q=1}^n \alpha_q = 1 \quad (3.3)$$

Interface shape and position identify accuracy of the VOF method. The interface between fluids is represented using a piecewise-linear approach in geometric reconstruction scheme. The geometric reconstruction scheme in Fluent is generalized for unstructured meshes from the work of Youngs (1982). It assumes that the interface between two fluids has a linear slope within each cell, and uses this linear shape for calculation of the advection of fluid through the cell faces. The first step in this reconstruction scheme calculates the position of the linear interface relative to the center of each partially-filled cell, based on information about the volume fraction and its

derivatives in the cell. The second step calculates the advection of the fluid through each face using the computed linear interface representation and information about the normal and tangential velocity distribution on the face. The third step calculates the volume fraction in each cell using the balance of fluxes calculated during the previous step (FLUENT, 2005).

The VOF method implemented in Fluent is only used with pressure based solutions. In the pressure-based approach, the pressure field is extracted by solving a pressure or pressure correction equation which is obtained by manipulating continuity and momentum equations (Patankar, 1980).

If the pressure field and face mass fluxes are known a velocity field can be obtained. Fluent uses a co-located scheme, whereby pressure and velocity are both stored at cell centers. However, the momentum equation requires the value of the pressure at the face. Therefore, an interpolation scheme is required to compute the face values of the pressure from the cell values. The default scheme Rhie and Chow (1983) in Fluent interpolates the pressure values at the faces using momentum equation coefficients. This procedure works well as long as the pressure variation between cell centers is smooth. When there are jumps or large gradients in the momentum source terms between control volumes, the pressure profile has a high gradient at the cell face, and cannot be interpolated using this scheme. In Fluent VOF modeling **Pressure Staggering Option (PRESTO)** scheme is highly recommended. The PRESTO scheme uses the discrete continuity balance for a “staggered” control volume about the face to compute the “staggered” (i.e., face) pressure. This procedure is similar in spirit to the staggered-grid schemes used with structured meshes, Patankar, 1980.

3.4 THE 2-D SIMULATION OF SLOTS

In order to get involve with FLUENT program at first a 2D model is constructed. This 2D model can represent slot type orifices that have an

infinite length. The geometrical properties of the 2-D model simulating flow in slots are represented in Fig 3.1.

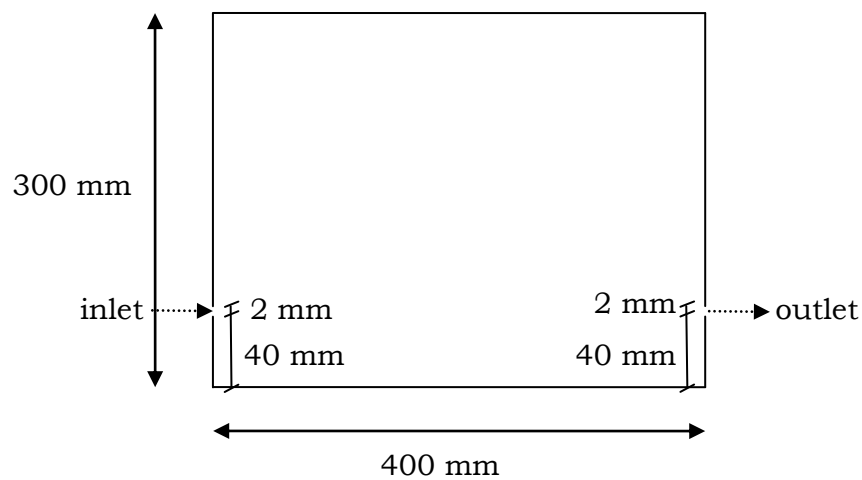


Figure 3.1: Geometrical properties of slots represented in 2-D

The 2-D flow is examined with two different meshes. The first mesh referred as coarse mesh has equal interval sizes; while the second one gets finer when gets closer to the plane passing through inlet and outlet and referred as fine mesh. The coarse mesh as can be seen in Fig 3.2 done with Quad elements and Map type with interval size 3 mm, this means height of one cell is bigger than the height of outlet and inlet opening. It consists of 13300 quadrilateral cells, 26367 interior faces of 2-D and 13534 nodes.

Whereas the fine mesh has been generated by meshing firstly the edges as summarized: The top and bottom edges are meshed with ratio 1.03 gets finer at the boundaries with interval count 120, the inlet and outlet edges has the ratio 1 and interval count 6 which means the outlet and inlet zones are divided to 6 cells, the edges below the inlet and outlet has ratio 1.04 with interval count 40 and gets finer closer to the inlet and outlet zones, and the edges above the inlet and outlet has ratio 1.02 with interval count 80 and gets finer closer to the inlet and outlet zones. All of the meshes of edges are successive ratio type. Then the face corresponding to the entire 2-D model is meshed in according to edge meshes and with Quad elements Submap type. The total mesh consists of 15120 quadrilateral cells, 29994 interior faces of 2-D, and 15367 nodes. It is presented in Fig 3.3.

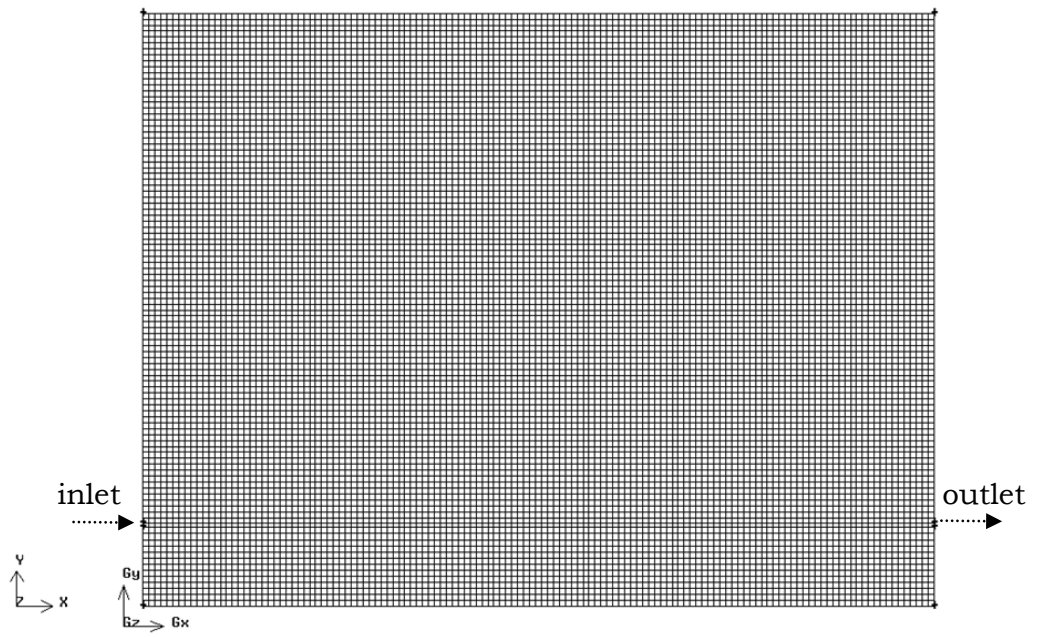


Figure 3.2: Coarse mesh for 2-D slot model

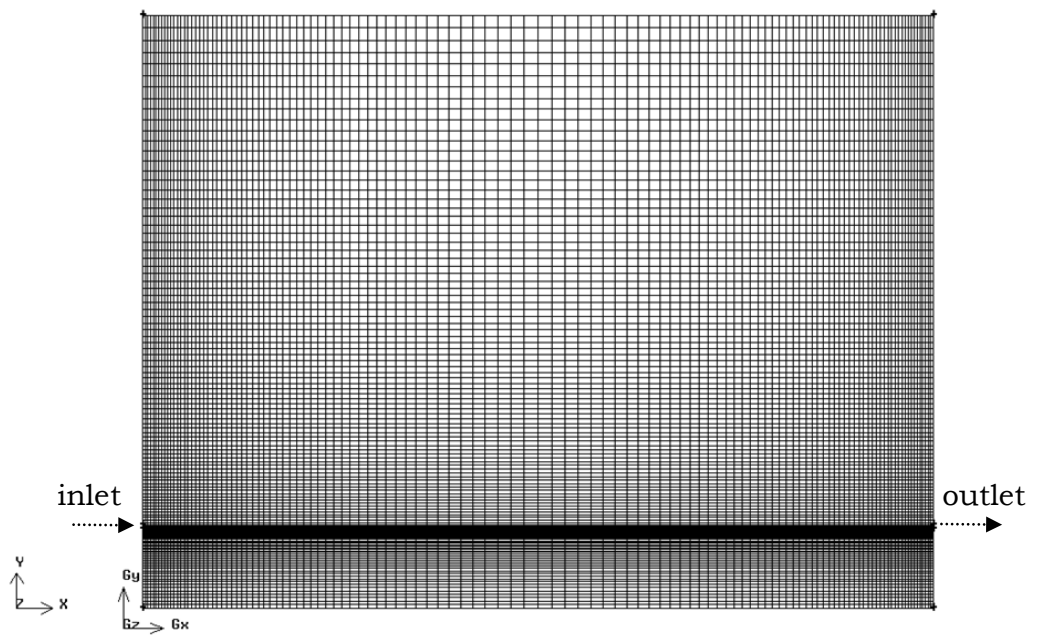


Figure 3.3: Fine mesh for 2-D slot model

In the simulation of slots three different models as laminar, standard $k-\epsilon$ and realizable $k-\epsilon$ turbulent are used.

Since the inlet is as the same geometry with the outlet, the water enters to the reservoir as a jet. So, the effects of the jet inside the reservoir do not disappear until the outlet as can be seen in Fig 3.4.

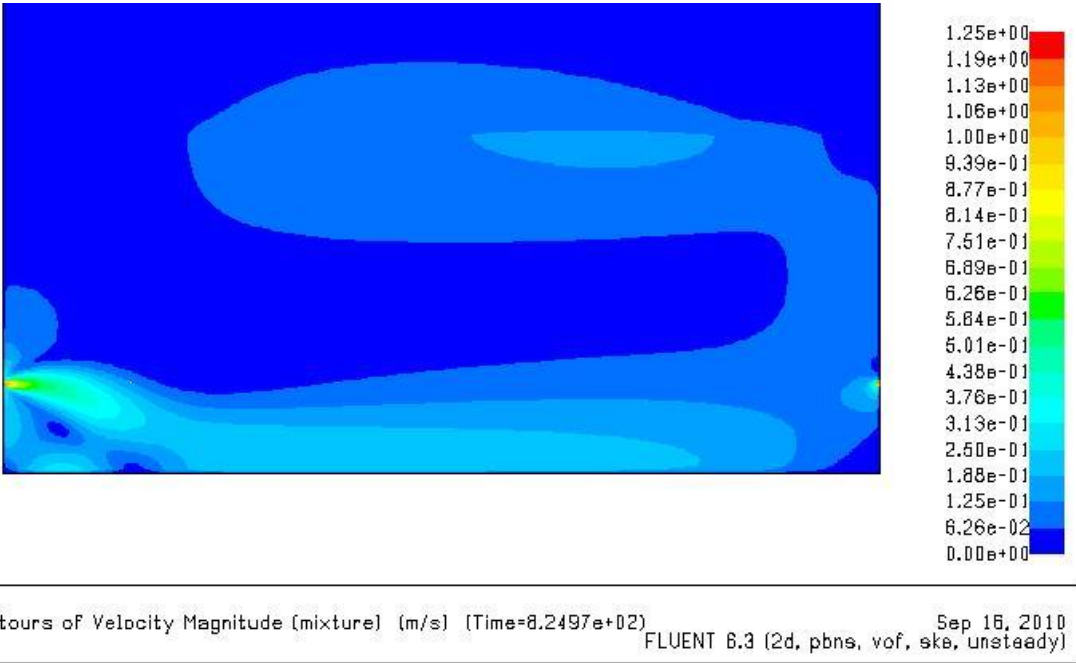
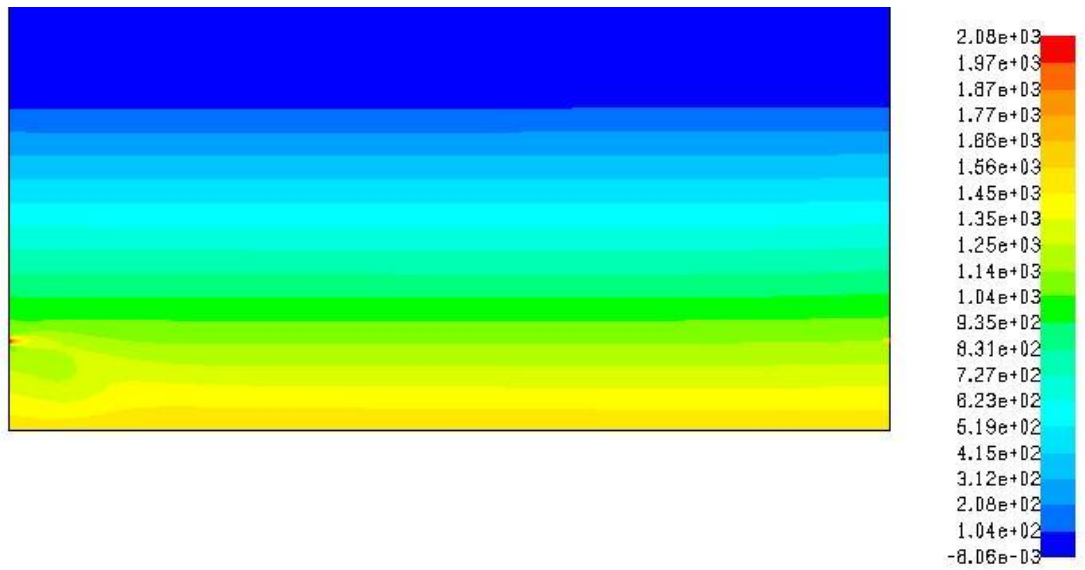


Figure 3.4: Velocity contours

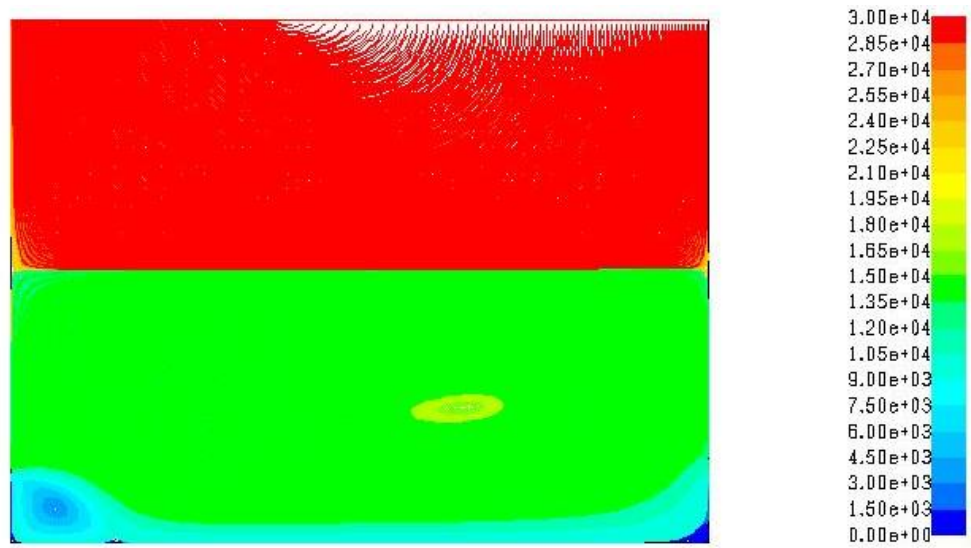
The total pressure contours show static distribution except for the inlet and outlet zones (Fig. 3.5).



Contours of Total Pressure (mixture) (pascal) (Time=6.2497e+02) Sep 16, 2010
 FLUENT 6.3 (2d, pbns, vof, ske, unsteady)

Figure 3.5: The total pressure contours

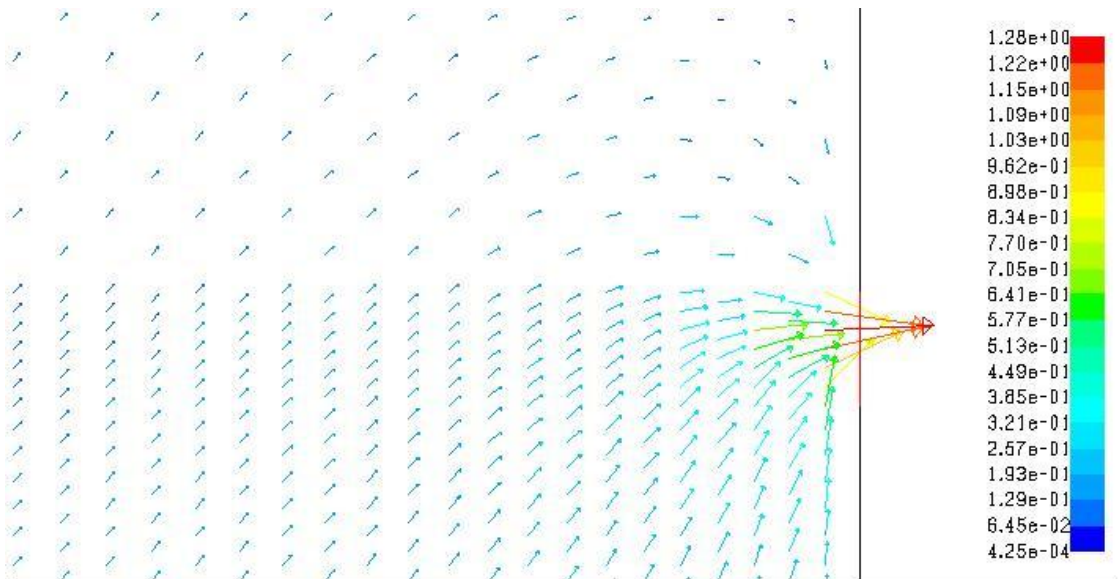
The pathlines inside the reservoir show that there is a vortex formation below the inlet, because of the high velocity (Figures 3.4 and 3.6). This effect will continue till the outlet and also reflects to the velocity vectors (Fig. 3.7).



Pathlines Colored by Particle ID (mixture) (Time=8.2497e+02)

FLUENT 6.3 (2d, pbns, vof, ske, unsteady) Sep 16, 2010

Figure 3.6: Pathlines inside of the reservoir



Velocity Vectors Colored By Velocity Magnitude (mixture) (m/s) (Time=8.2497e+02)

FLUENT 6.3 (2d, pbns, vof, ske, unsteady) Sep 16, 2010

Figure 3.7: Velocity vectors close to the outlet

CHAPTER 4

FLOW SCRUTINIZATION

4.1 GENERAL INFORMATION

In this chapter the flow characteristics through orifices are presented. Two different orifices, namely sharp crested orifice and tube orifice, connected to a tank are modeled by FLUENT program. The results are compared with both available theoretical and experimental studies in the literature. Discussions on the representative dimensions of the problems are introduced. Further, type of the flow within the tank, whether it is inviscid, laminar or turbulent, is discussed.

4.2 PHYSICAL MODEL

Çobanoğlu (2008) conducted experiments in order to establish a relation of the Reynolds number and discharge coefficient as described in Chapter 2. As a follow up of Çobanoğlu's (2008) study, physical model is chosen to be the

same as in that study. The tank has a 400 mm height, 370 mm length and 470 mm width. In Fig. 4.1 orientations of the outlet on the face of the tank can be seen. Although Çobanoğlu has conducted the experiments for all the outlets which are shown in the figure, only the middle one of the vertical axis is used in this study since this outlet has a symmetry along the transverse direction, therefore it will be more suitable while comparing other studies in the laboratory. The most bottom outlet is very near to the solid boundary and it is very difficult to collect experimental data for such an outlet. In addition, the upper outlet is not chosen in order to decrease the computational domain size.

The various scenarios are composed in order to have detailed discussion on the results.

1) Mesh effect: Two different meshes of the tank, namely coarse and fine are constructed in order to see the mesh effect.

2) Flow type: Simulation of inviscid, laminar and turbulent flows are done.

There is limited number of studies to observe flow behavior at the upstream of simple orifices. To our knowledge, there is no any study for orifice tubes. Therefore, the same tank is modeled with a simple orifice in order to validate results with available studies.

composed of 91914 mixed cells, 178688 triangular interior faces and 18019 nodes.

The reason that the interval size for outlet is kept constant and small is from the conclusion that the outlet geometry is very small related to tank and the computations in the outlet is very important due to the change of flow type as discussed in the Section 3.2. Therefore, it should be represented with finer and outnumbering meshes.

The boundary zones of the model are defined as in the Fig. 4.4 in the GAMBIT. The inlet boundary type is set as mass flow inlet as seen the grey zone in the figure, and the outlet boundary types are set as pressure outlets which are corresponding to the top of the reservoir and the outlet face of the sharp crested orifice seen as red zones in the figure.

The steady state discharge of the system is $Q= 36.98 \text{ cm}^3/\text{s}$.

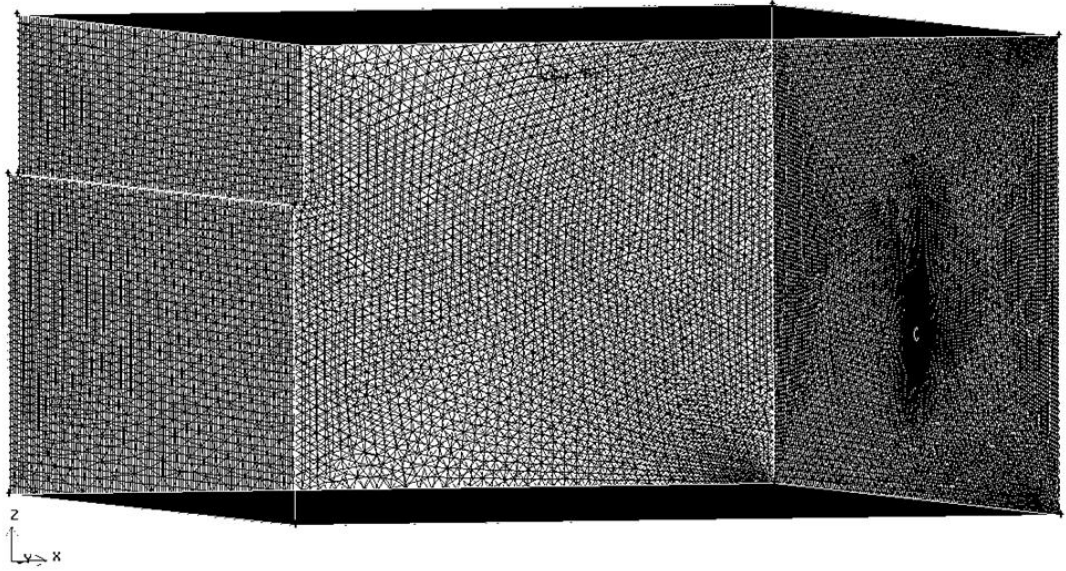


Figure 4.2: Fine mesh for sharp crested orifice

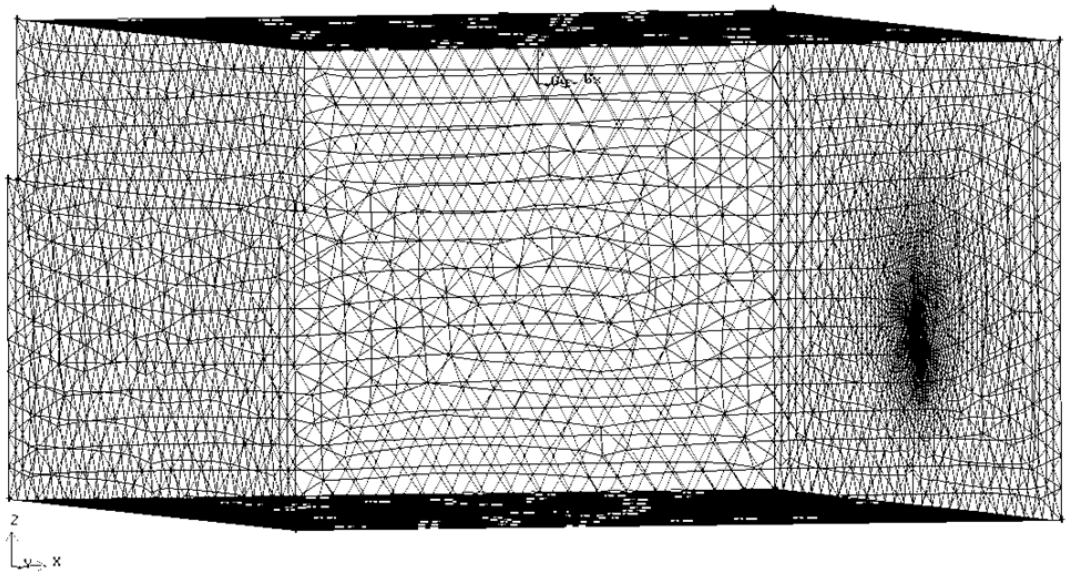


Figure 4.3: Coarse mesh for sharp crested orifice

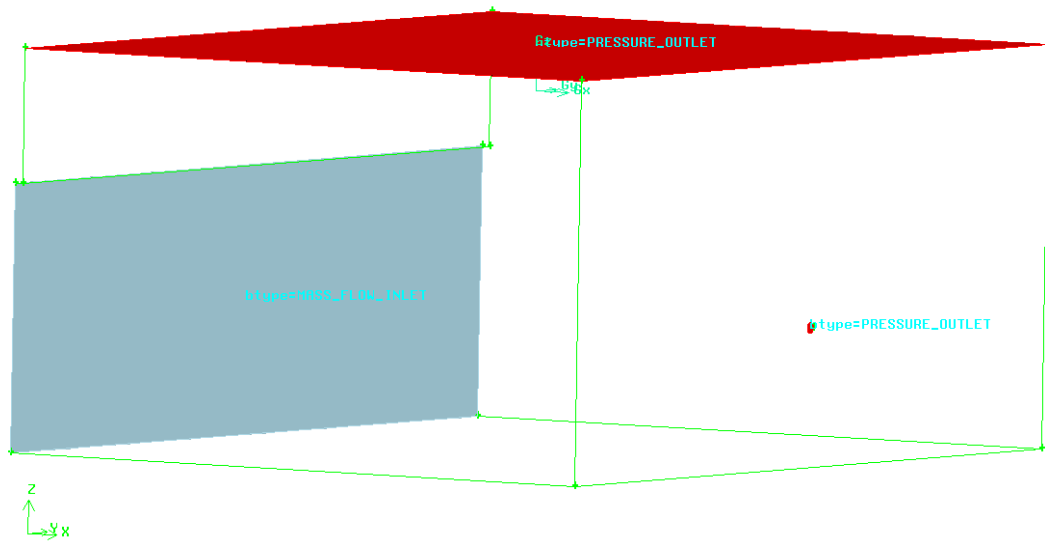


Figure 4.4: Boundary types of the model

The results of the simulations are compared with Bryant et al. (2008). Figures 4.5, 4.6 and 4.7 present the experimental data of Bryant et al.(2008), potential flow solution of them and inviscid and turbulent solution of FLUENT. The centerline velocities of this study corresponds to the computational nodes within the distance $x/d=3$. It can be seen from Figures 4.5 and 4.6 that both fine and coarse mesh gives reasonable results, the mesh effect did not play an important role in these comparisons. It is concluded that the finer mesh is not always the better; the mesh should be optimized for accuracy and time. The inviscid solution cannot predict centerline velocity in the vicinity of the outlet. Therefore laminar and turbulent models are also tried. All those results of the models will also be discussed with the results of the orifice tubes.

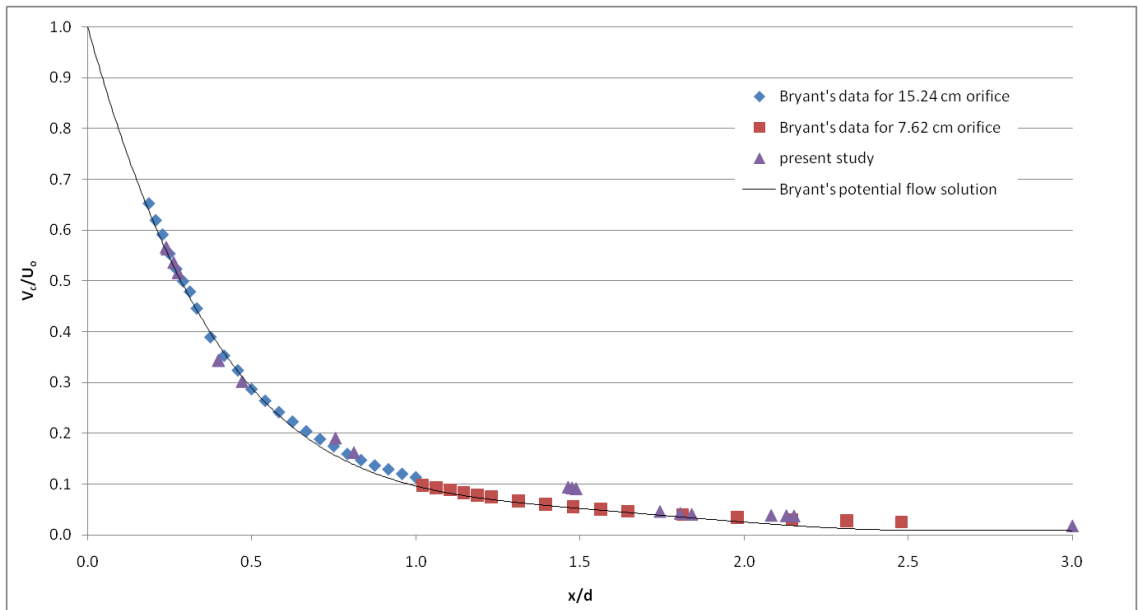


Figure 4.5 Comparison of centerline velocity profile for sharp crested orifice inviscid flow solution with fine mesh

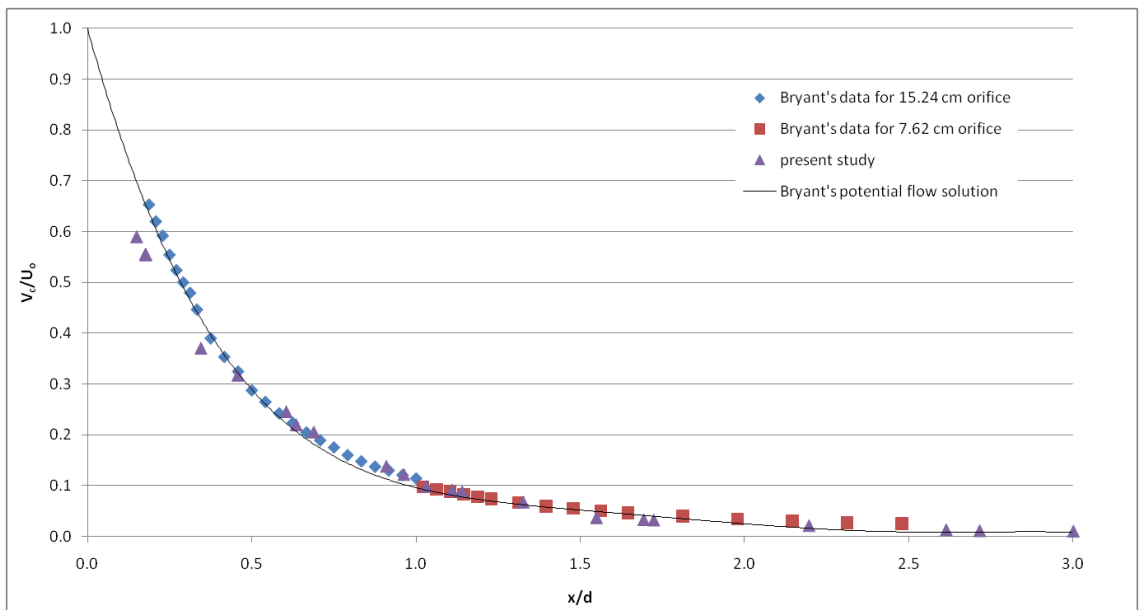


Figure 4.6: Comparison of centerline velocity profile for sharp crested orifice inviscid flow solution with coarse mesh

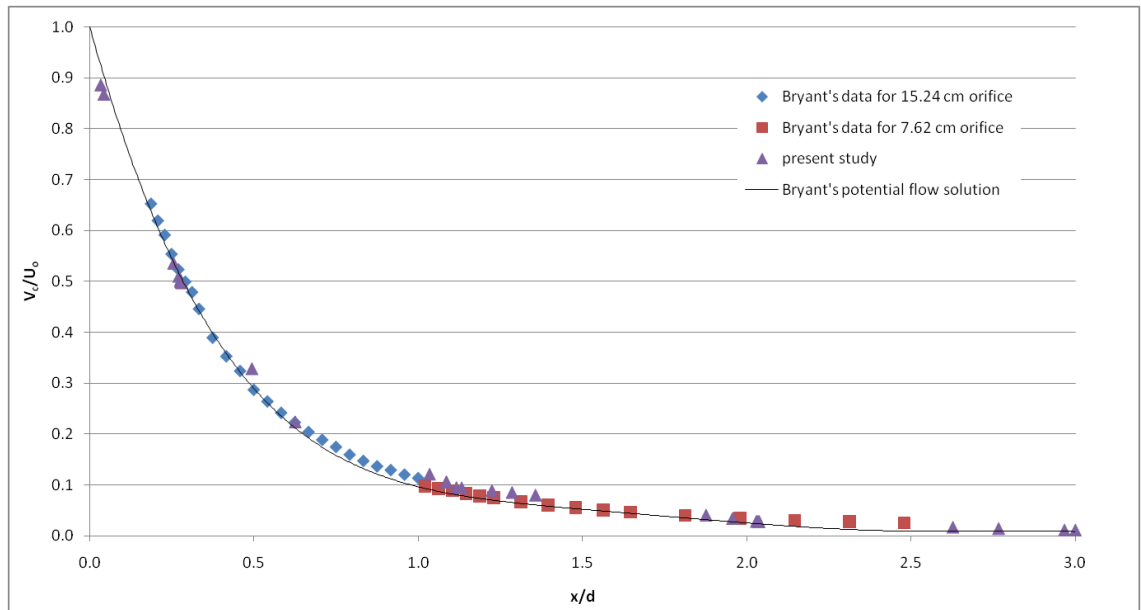


Figure 4.7: Comparison of centerline velocity profile for sharp orifice turbulent flow solution with coarse mesh

4.2.2 CIRCULAR TUBE ORIFICES

The orifice tube simulations have done with the coarse mesh since it is concluded that the mesh effect did not play an important role as discussed in Section 4.2.2. The ℓ/d ratio for the orifice tubes is 5.

The tank and orifices are meshed by using GAMBIT program. The mesh can be seen in Fig 4.8. , The mesh of the model is composed of 68252 nodes, 657010 mixed interior faces and 333723 mixed cells.

A finer mesh is chosen in the outlet pipe since it is a small geometry compared to the. The mesh of the face of orifice pipe is generated by Quad

elements and Pave type with interval size 1 mm. The rest of the volume mesh is generated by Tet/Hybrid elements and Tgrid type with interval size of 15 mm. The boundary types are assigned as seen in Fig. 4.9. Mass flow inlet boundary condition is assigned to the inlet face and pressure outlet boundary condition is assigned to the top and pipe outlet faces.

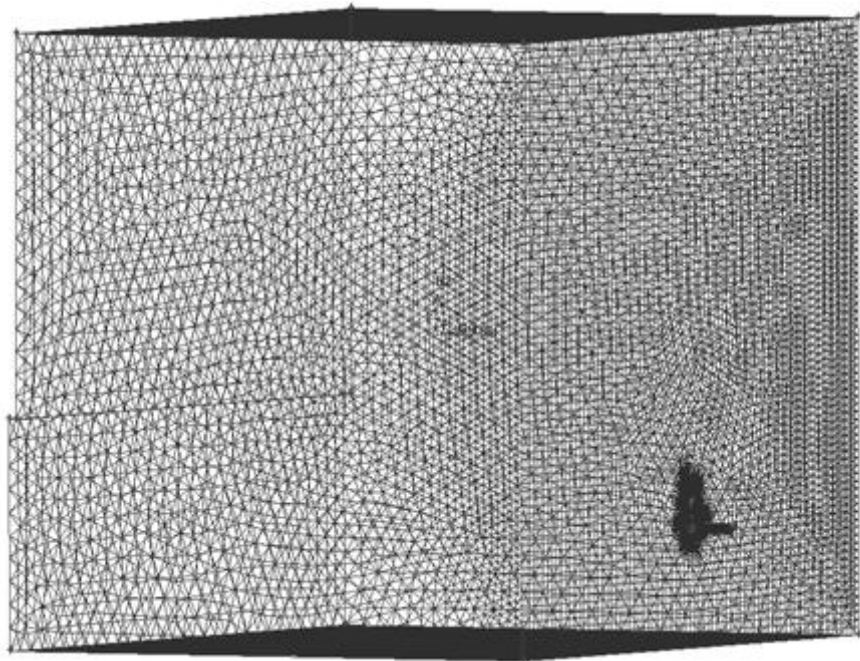


Figure 4.8: General view of the tank model

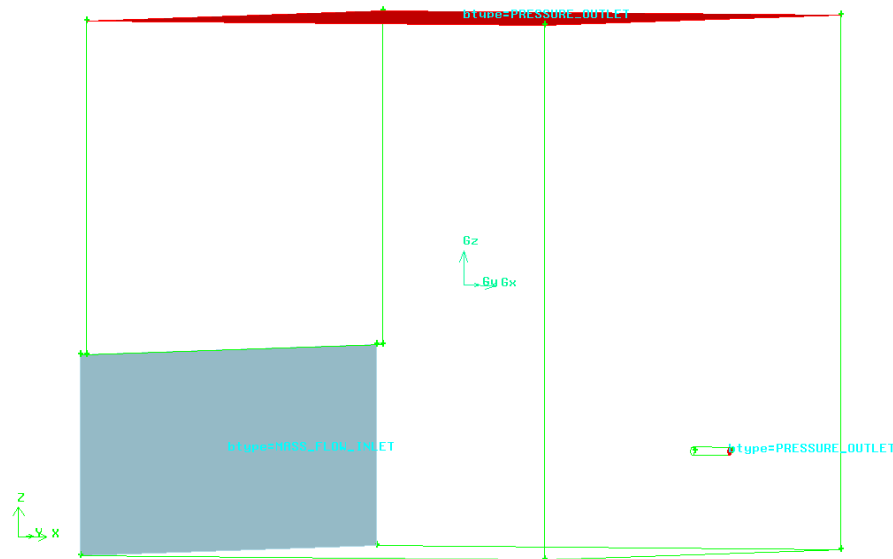


Figure 4.9: Boundary conditions for orifice tube

There are plenty of results that can be produced by using computational fluid dynamics, here; some selective results are presented, such as velocity field and pressure field, since there is lack of experimental study to compare the results. One may measure velocity field and the pressure field within the tank, but it is very difficult to get measurement within the tube. It should be noted that the velocity profile within tube is changing along the pipe axis due to boundary layer development. Therefore, a very simple check was made by using orifice discharge coefficients.

After, the solution reached to the steady state solution the water depth over the outlet and the value of the mass flux of the outlet (\dot{M}) is obtained from the results. Then ideal velocity (v) is computed from the head over the orifice (H) and real velocity (V) is computed by dividing the outlet discharge (Q_{out}) to the cross sectional area. The discharge coefficient, C_d and Reynolds number, Re is also calculated as discussed in Section 2.2.2. Thus the model is treated as an experimental set-up. Table 4.1 is constructed

accordingly for all of the models developed within the study. These discharge coefficients are compared with the experimental results of Çobanoğlu (2008) as seen Figure 4.10. In this figure data of Ramamurthi and Nandakumar (1999) are also compiled.

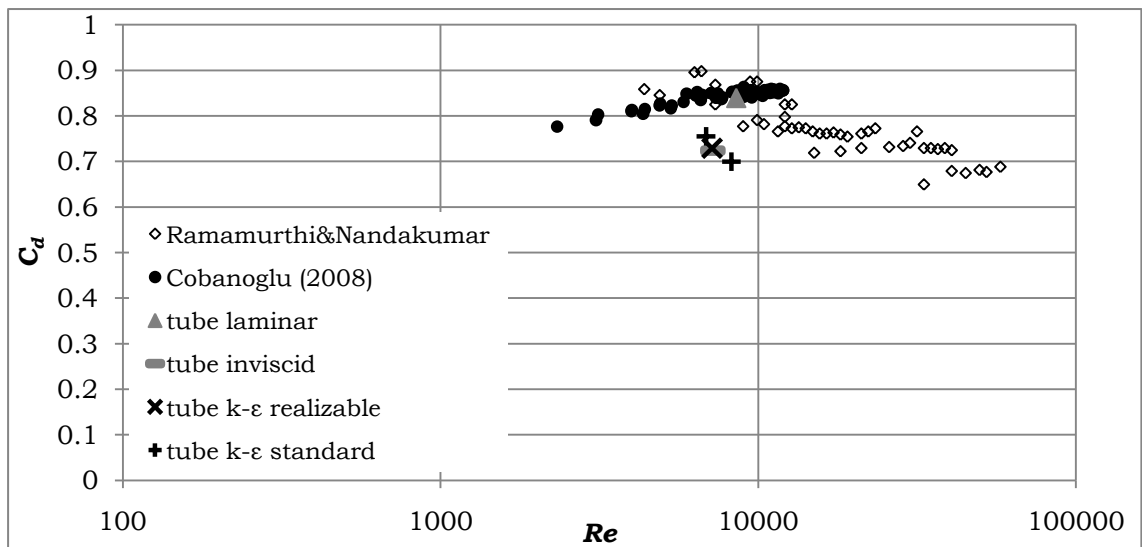


Figure 4.10: Re versus C_d graph for various data and cases

In table 4.1; 19 runs that carried out within this study are presented. The first three rows of the table referred as Case 1 corresponds to the simulations of sharp crested orifice with coarse mesh and the following two rows referred as Case 2 are for the same orifice with fine mesh. As can be seen from the table the discharge coefficient, C_d values of Case 1A and Case 1C shows similarity, so inviscid solution can represent the flow.

The rows between 6th and 10th are referred as Case 3 and correspond to simulation of circular tube orifices with coarse mesh. As can be seen from Figure 4.9, the laminar flow best represents the flow among the others. Since, the discharge coefficient, C_d values of the others do not fit with the experimental results.

In the rows between the 11th and 14th of the table, one can see the results of 2-D model, that renamed as slot type orifice, with fine mesh and referred as Case 4 and the last 5 rows of the table represents the coarse mesh for 2-D slots.

Table 4.1: A summary of all the runs

Case	Model	Type of orifice	Type of Mesh	H (m)	d or a (m)	R (m)	\dot{M}_{out} (kg/s)	Q_{out} (m ³ /s)	v (m/s)	V (m/s)	C_d	Re
1A	3D inviscid	sharp	coarse	0.1425	0.006	0.0015	0.0348	3.48E-05	1.6721	1.2311	0.7363	7353.51
1B	3D laminar	sharp	coarse	0.1425	0.006	0.0015	0.0362	3.62E-05	1.6721	1.2815	0.7664	7654.41
1C	3D k- ϵ standard	sharp	coarse	0.1400	0.006	0.0015	0.0351	3.52E-05	1.6573	1.2449	0.7512	7436.00
2A	3D inviscid	sharp	fine	0.1475	0.006	0.0015	0.0347	3.48E-05	1.7012	1.2300	0.7231	7347.05
2B	3D laminar	sharp	fine	0.1475	0.006	0.0015	0.0360	3.61E-05	1.7012	1.2766	0.7504	7625.31
3A	3D inviscid	tube	coarse	0.1413	0.006	0.0015	0.0340	3.41E-05	1.6647	1.2049	0.7238	7197.08
3B	3D laminar	tube	coarse	0.1475	0.006	0.0015	0.0403	4.04E-05	1.7012	1.4275	0.8391	8526.57
3C	3D k- ϵ standard	tube	coarse	0.1400	0.006	0.0015	0.0327	3.27E-05	1.6573	1.1568	0.6980	6909.86
3D	3D k- ϵ standard	tube	coarse	0.1975	0.006	0.0015	0.0389	3.89E-05	1.9685	1.3774	0.6997	8227.49
3E	3D k- ϵ realizable	tube	coarse	0.1375	0.006	0.0015	0.0338	3.39E-05	1.6425	1.1977	0.7292	7154.14
4A	2D k- ϵ standard	slot	fine	0.0330	0.002	0.0010	1.3586	1.36E-03	0.8046	0.6803	0.8455	2703.62
4B	2D k- ϵ standard	slot	fine	0.0780	0.002	0.0010	2.0623	2.07E-03	1.2371	1.0327	0.8348	4104.05
4C	2D k- ϵ standard	slot	fine	0.1180	0.002	0.0010	2.5071	2.51E-03	1.5216	1.2554	0.8251	4989.18
4D	2D k- ϵ standard	slot	fine	0.1200	0.002	0.0010	2.4978	2.50E-03	1.5344	1.2508	0.8152	4970.78
5A	2D k- ϵ realizable	slot	coarse	0.0120	0.002	0.0010	0.9048	9.06E-04	0.4852	0.4531	0.9338	1800.68
5B	2D k- ϵ standard	slot	coarse	0.0110	0.002	0.0010	0.9035	9.05E-04	0.4646	0.4524	0.9739	1798.00
5C	2D k- ϵ realizable	slot	coarse	0.0450	0.002	0.0010	1.7999	1.80E-03	0.9396	0.9013	0.9592	3581.87
5D	2D k- ϵ realizable	slot	coarse	0.0450	0.002	0.0010	1.8056	1.81E-03	0.9396	0.9042	0.9623	3593.27
5E	2D laminar	slot	coarse	0.0115	0.002	0.0010	0.9133	9.15E-04	0.4750	0.4573	0.9628	1817.43

4.3 POST PROCESSING OF THE SOLUTIONS

Post processing of the solutions is done by choosing two cases namely Case 1A and Case 3B for the sharp crested orifices and the circular pipe orifices, respectively.

4.3.1 SHARP CRESTED ORIFICES

The various results for the sharp crested orifice of Case 1A corresponding to the inviscid flow with coarse mesh is presented in this section.

The velocity contours that colored with velocity magnitude is as seen in Figure 4.11. The velocity at the outlet of a sharp orifice is not uniform and it differs from 1.23×10^{-5} m/s to 1.41 m/s from boundaries to the center. Also as can be seen on Figure 4.12; the total pressure also differs from 1.21 kPa to 1.53 kPa. Thus, neither the velocity nor pressure is uniformly distributed across the cross-section. So that the atmospheric pressure assumption in outlet zones are not correct. Figure 4.13 shows the velocity field upstream of the sharp crested orifice. Acceleration of the flow due to orifice opening can be clearly observed.

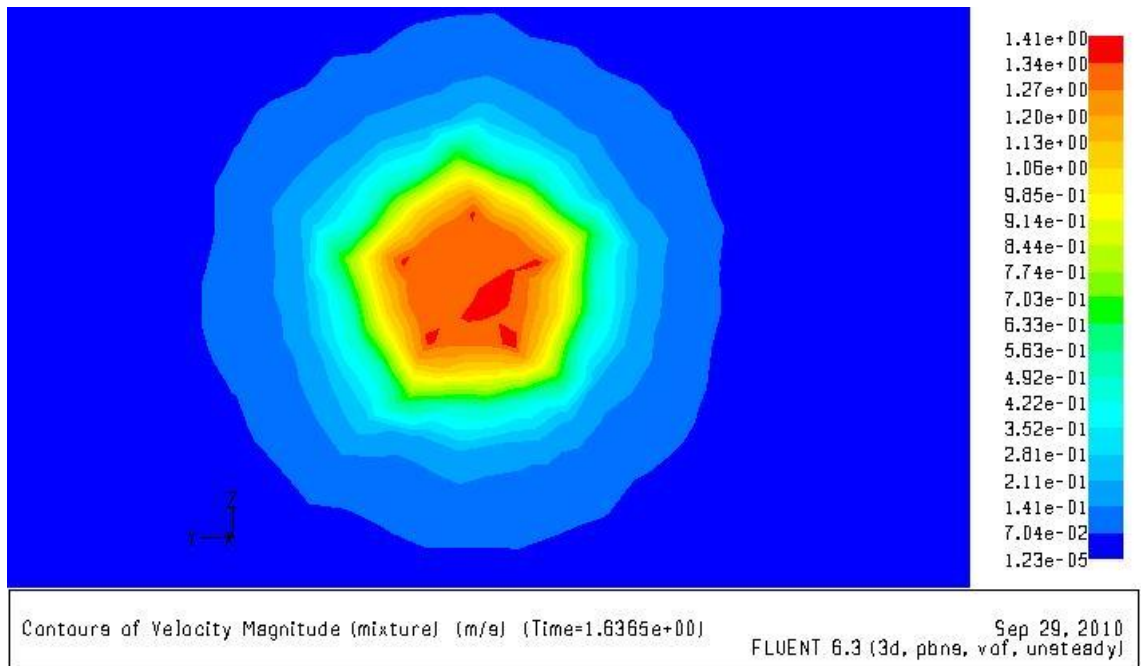


Figure 4.11: Velocity Contours of Case 1A

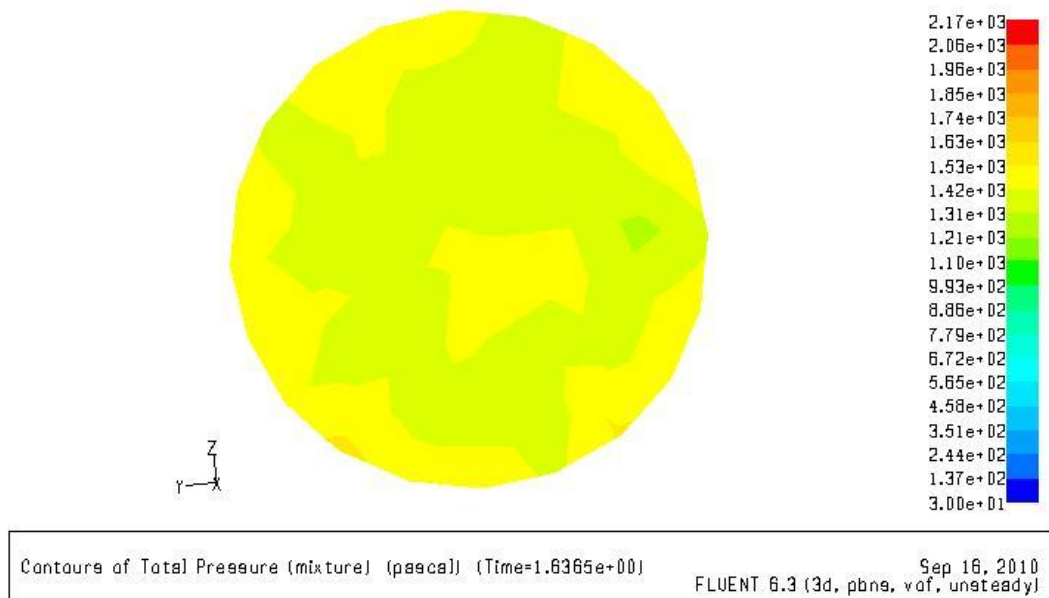


Figure 4.12: Total Pressure Contours of Case 1A

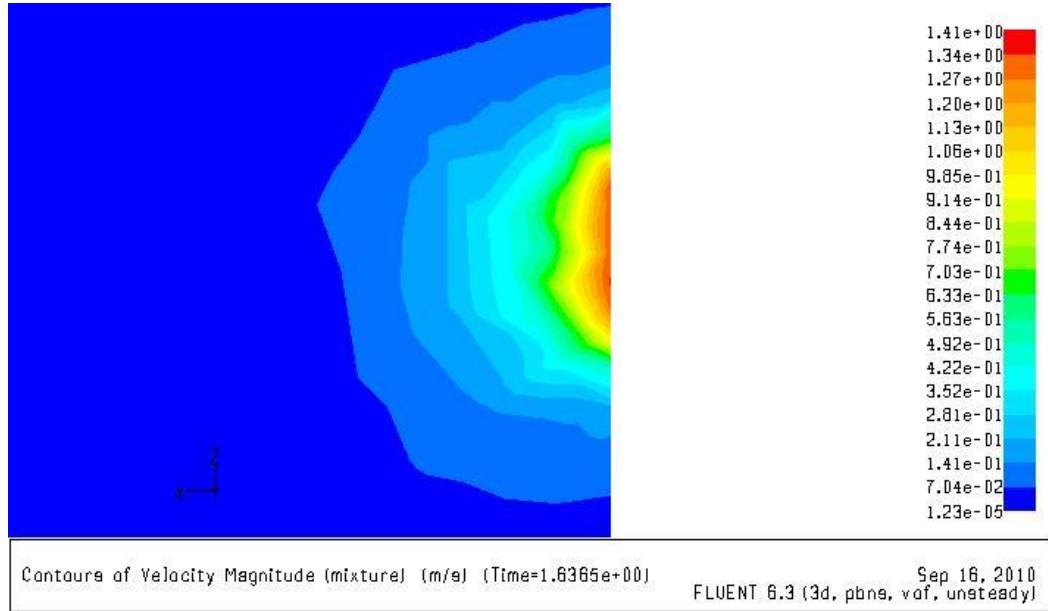


Figure 4.13: Contours of velocity of case 1A side

4.3.2 CIRCULAR TUBE ORIFICES

The laminar case 3B is an example of simulating the model of the orifice tube. The velocity contours of the outlet are presented in Figure 4.14 and Figure 4.15. The velocity contours are not perfectly rounded because of the mesh, the better result can be obtained with a finer one (Fig. 4.15). The velocity profile changes from 0 to 1.98 m/s from boundary to the center of the pipe. The backward effect of the orifice flow can be seen in a distance approximately $1d$ below and over the orifice and $2d$ behind it as can be seen in Figure 4.16.

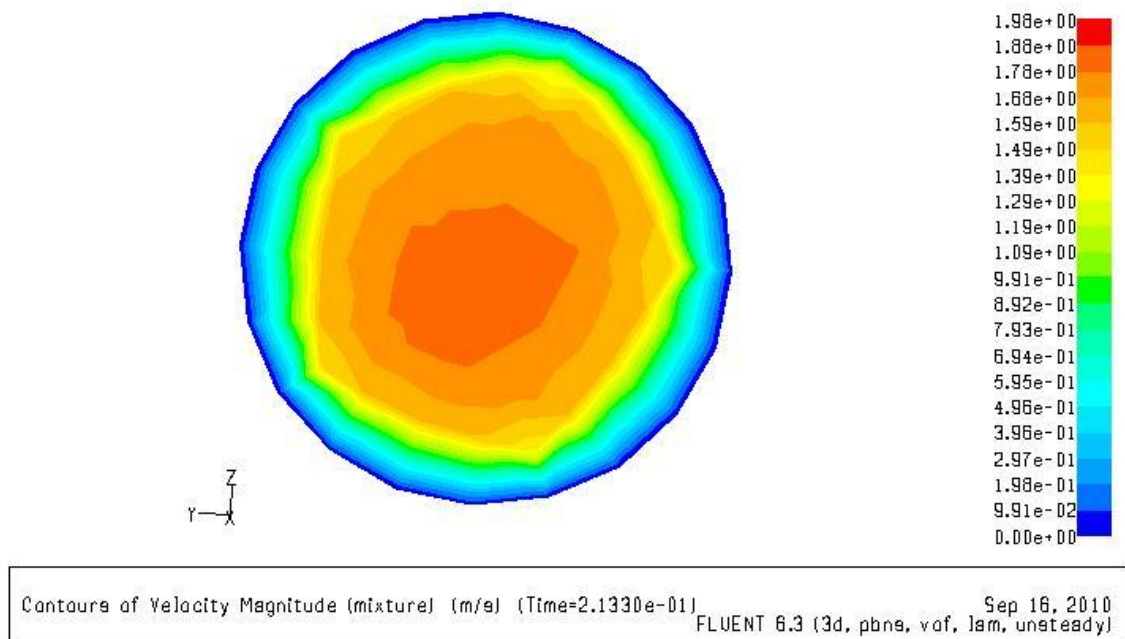


Figure 4.14: Velocity contours of the outlet for case 3B

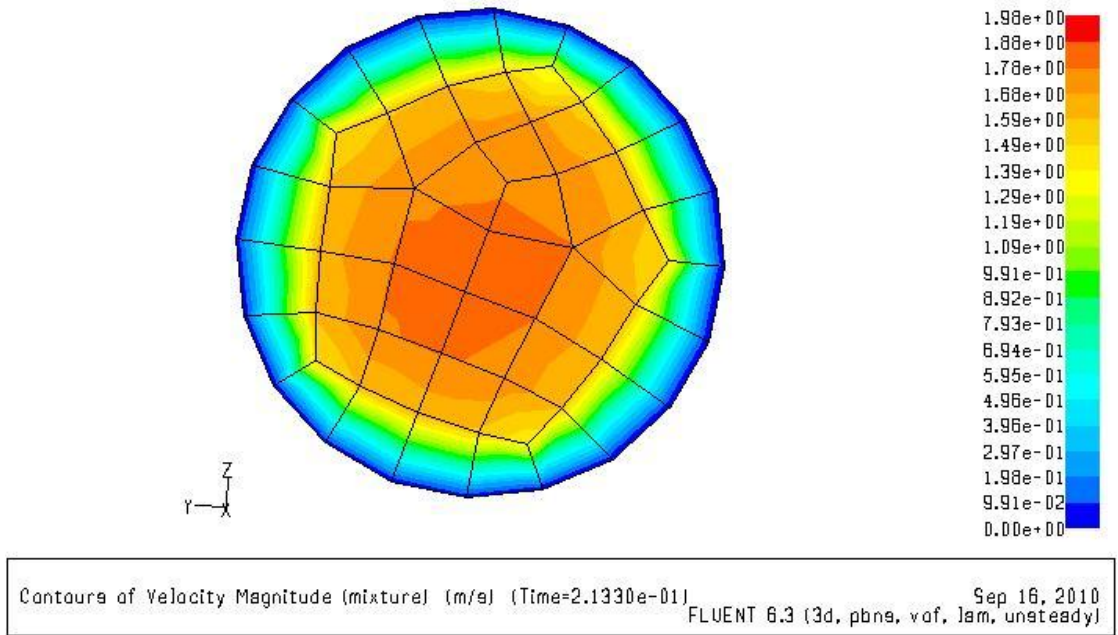


Figure 4.15: Velocity contours of the outlet with grid for case 3B

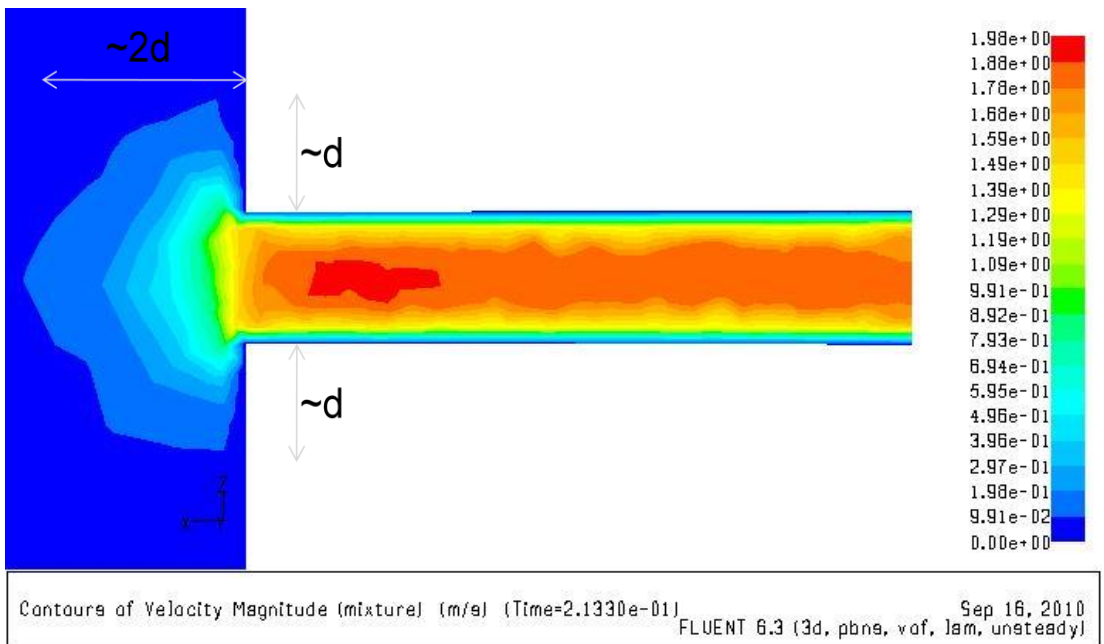


Figure 4.16: Velocity contours for the centerline of the tube for case 3B

As stated in Section 4.2.2 the calculations ended when the flow is reached to the steady state. So, the mass flux rate of the outlet and the residuals

are checked in order to decide that flow is steady anymore. The calculation process is continued until the mass flow rate gets steady as Figure 4.17, since, it is the mass flux of the outlet it is denoted by negative sign(-) and the residuals are checked in order to be equal or under the magnitude of 10^{-4} as seen in Figure 4.18. The flow time is 0.2133 s for this case.

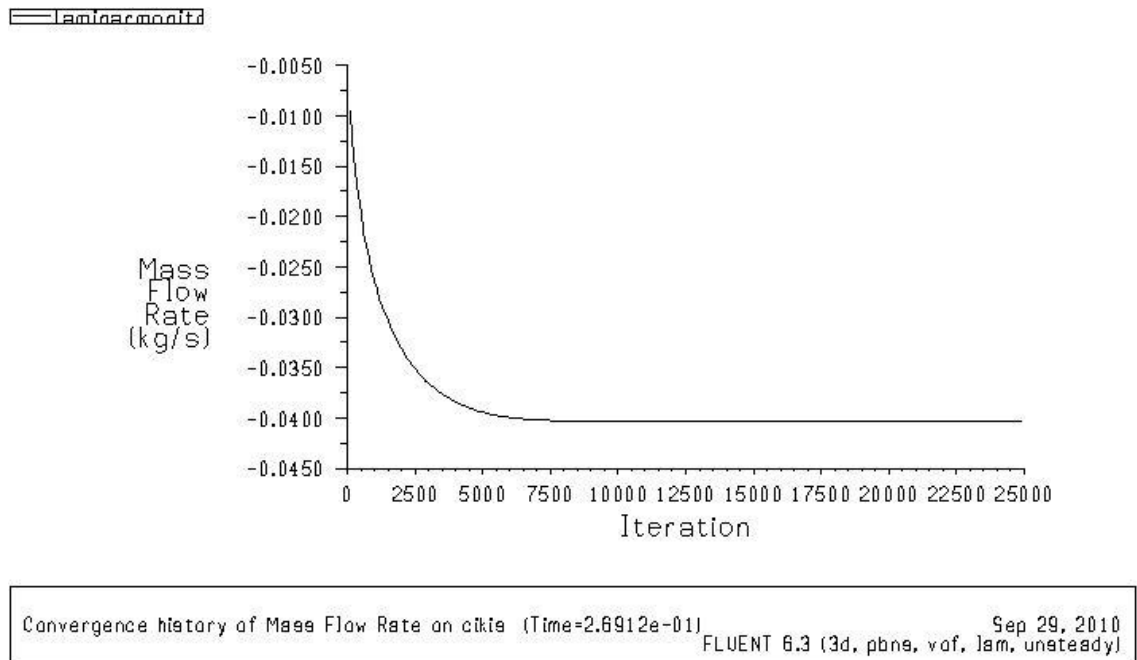


Figure 4.17: Mass flow rate versus Iteration on outlet for Case 3B

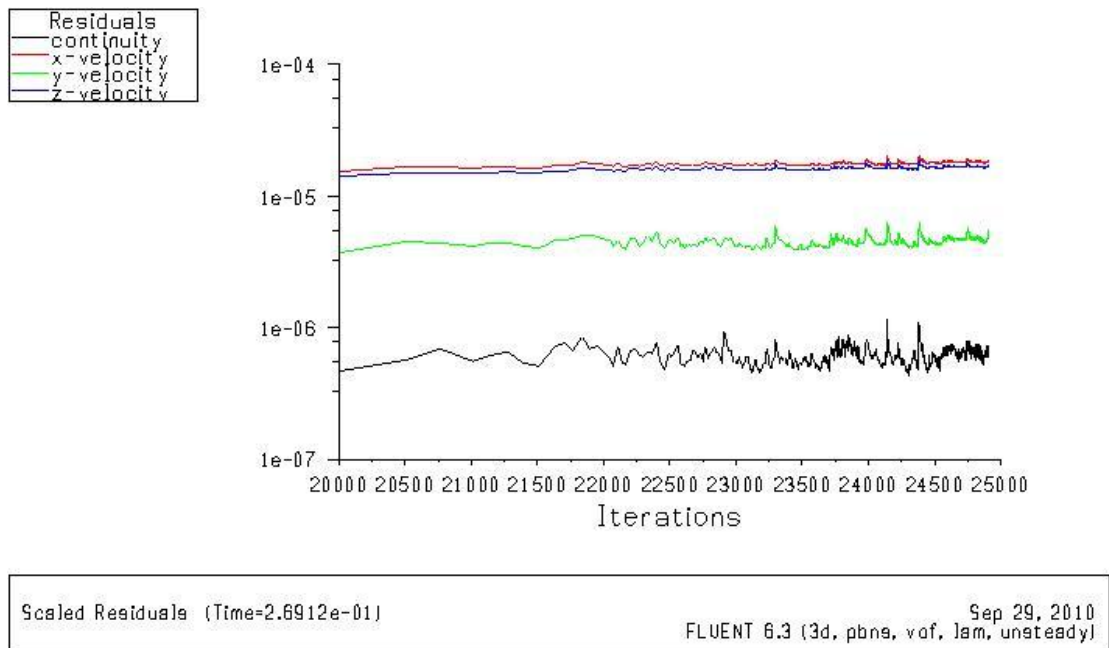


Figure 4.18: Residuals for Case 3B

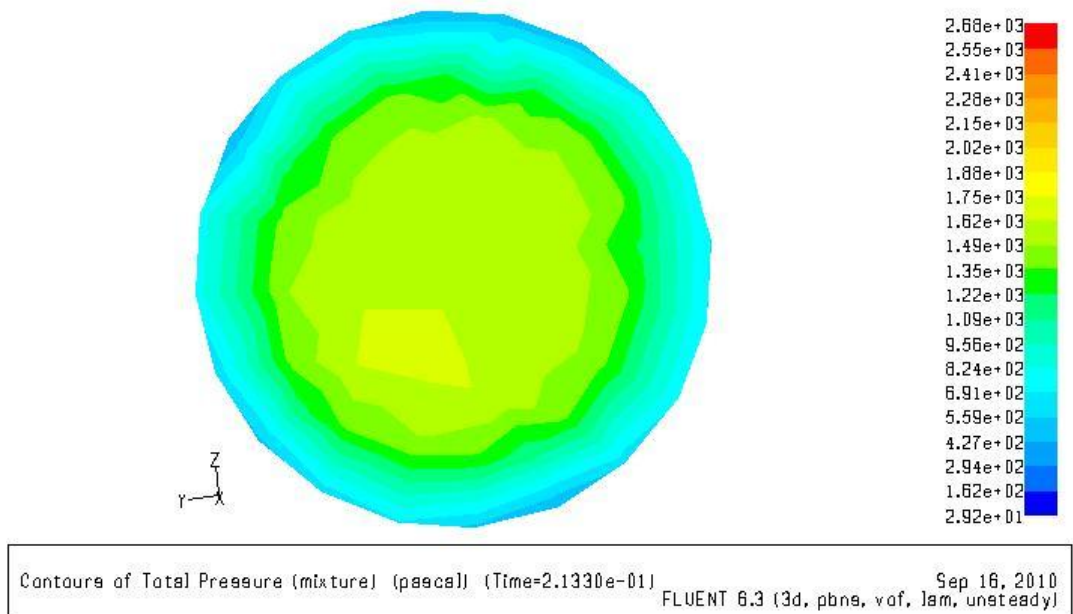


Figure 4.19: Contours of Total Pressure on outlet for Case 3B

The pressure contours of the model and the outlet can be seen in Figure 4.19 for the cross section and in Figure 4.20 for the longitudinal section. Zero pressure is achieved in the vena contracta and can be seen in Figure 4.21. As discussed in Section 4.3.1 that the assumption of atmospheric pressure at the outlet is not valid for this case also.

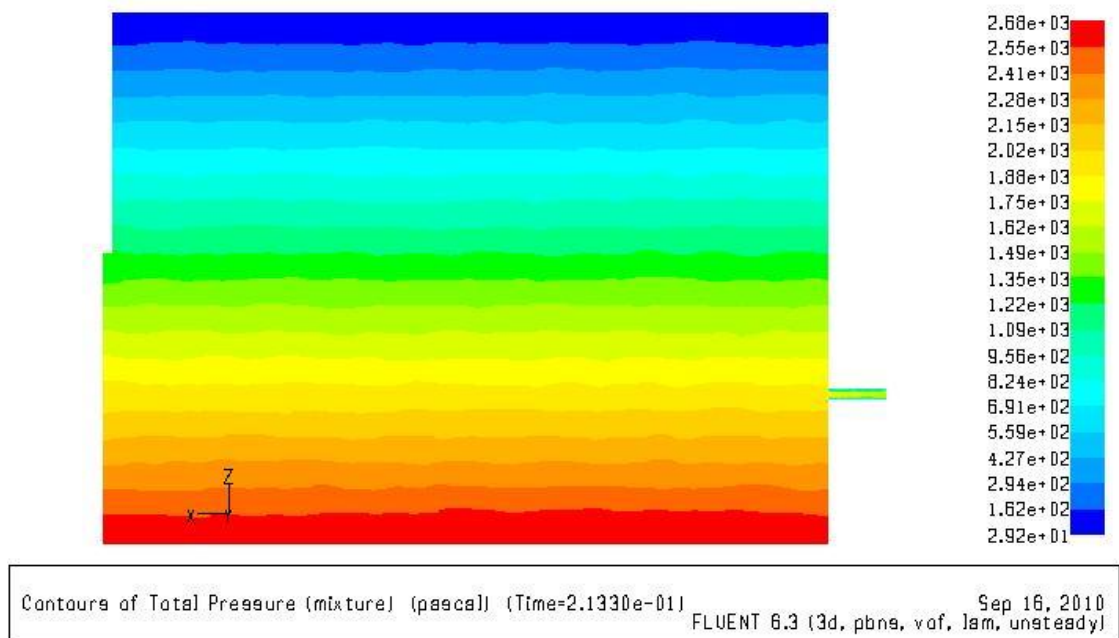


Figure 4.20: Contours of Total Pressure for Case 3B

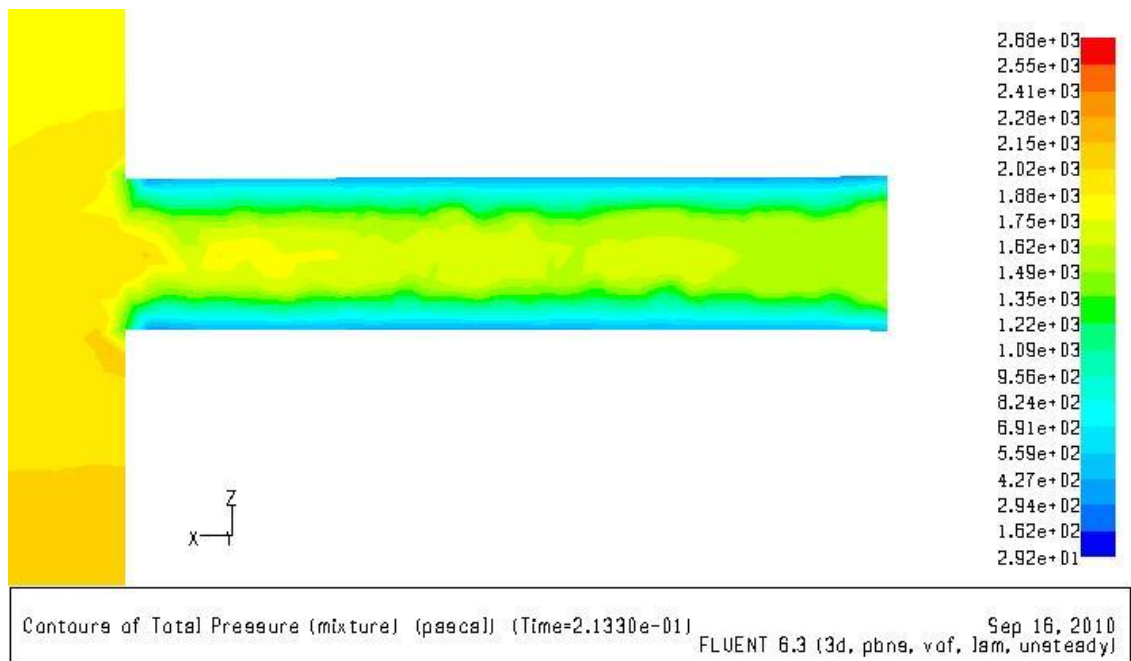


Figure 4.21: Contours of total pressure on the tube for Case 3B

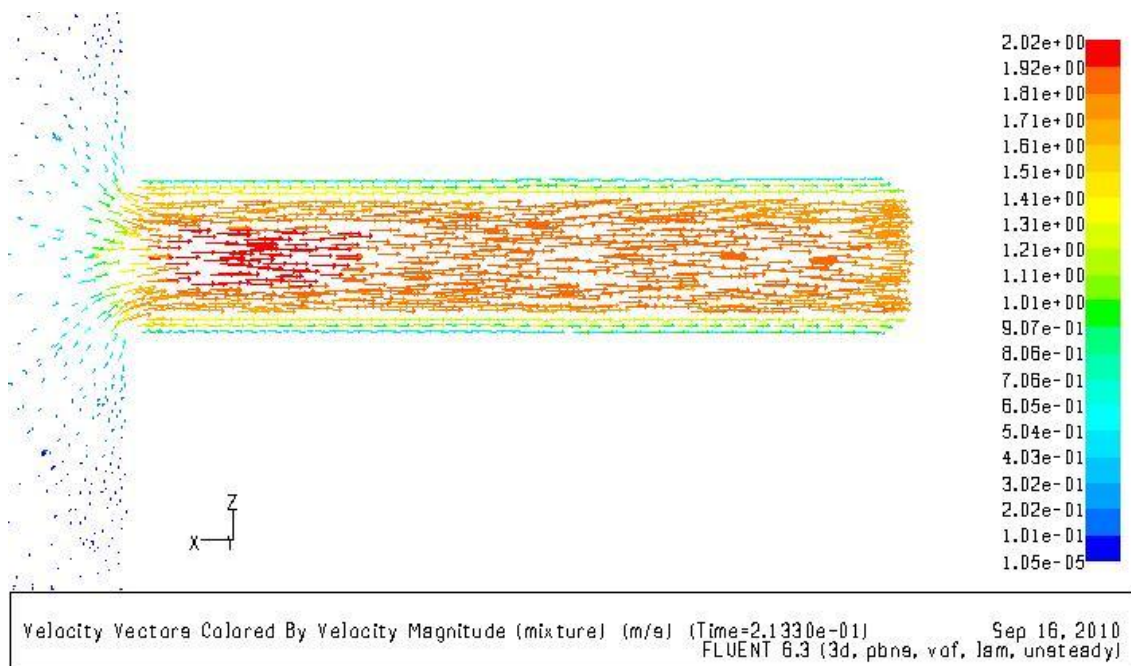


Figure 4.22: Velocity vectors in the tube for Case 3B

The Figures 4.22 and 4.23 shows that the velocity profile is not getting uniform for $\ell/d = 5$, so the length is not enough for a fully developed flow. Actually in the literature the entrance length to pipe diameter is defined for

both laminar and turbulent flows, as given in Eq. 4.1 and 4.2, respectively (Munson et al. 1998).

$$\ell_e / d = 0.06 Re \tag{4.1}$$

$$\ell_e / d = 4.4 Re^{1/6} \tag{4.2}$$

where ℓ_e corresponds to the entrance length. For the case evaluated here corresponding to approximately the Reynolds number of 8000, thus

$$\ell_e / d \approx 20$$

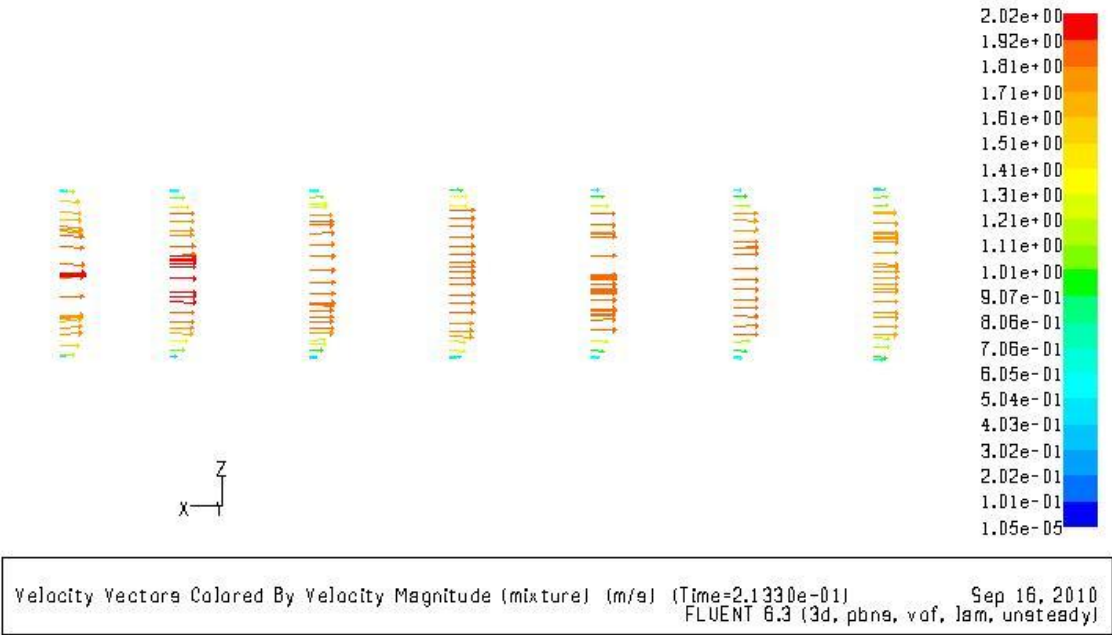


Figure 4.23: Velocity vectors for every 5 mm of tube for Case 3B

CHAPTER 5

CONCLUSION

In this study, flows at the upstream of an orifice and through orifice are analyzed. It shows that numerical solution is a must to obtain flow field in an intake structure. The analytical solutions are not capable in every quantity such as velocity and pressure distributions. Further there are limitations for experimental studies, too. The followings are deduced from the results of the numerical model:

1) The flow at the upstream of an orifice can be accepted inviscid except in the vicinity of the outlet. The comparison of the simulation with the potential flow solutions shows that potential flow solution describes the velocity flow well except the zone nearby orifice opening. In close proximity where the experimental data cannot be found, the potential flow solution is also not accurate.

2) The result of laminar flow modeling can be used to calculate discharge coefficient of the orifice tube if the state of the flow is in the transient region ($Re=2000\sim 10000$). There will not be a fully developed flow unless the orifice length to diameter ratio is greater than 20.

3) The orifice flow is investigated and that the coefficient of discharge value is an important factor in understanding of flow. It shows that the analysis

of FLUENT model results fall in the same range of the experimental data. This shows the reliability of the software.

The results can be obtained for different Reynolds number cases in future studies, so that a broad data for C_d can be achieved. Also the solutions should be enlarged for different length to diameter ratio.

REFERENCES

- ANSYS, Fluent Inc., www.fluent.com, last visited on 30 August 2010.
- Aydın, I., Altan-Sakarya, A.B. and Ger, M., (2006). Performance of Slit Weir. *J. of Hydraulic Engineering, ASCE* 132(9): 987-989.
- Bos, M.G., (1989). Discharge Measurement Structures, International Institute for Land Reclamation and Improvement, Wageningen, The Netherlands; ISBN 90 70754 150.
- Borutzky, W., Barnard, B. and Thoma, J., (2002). An orifice flow model for laminar and turbulent conditions. *Simulation Modelling Practice and Theory*, 10: 141-152.
- Brater, E.F. and King, H.W., (1982). Handbook of Hydraulics for the Solution of Hydraulic Engineering Problems, USA. 2; ISBN 0-07-007243-4.
- Bryant, D.B., Khan, A.A. and Aziz, N.M. (2008). Investigation of flow upstream of orifices. *Journal of Hydraulic Engineering*, 134(1), 98-104.
- Cevheri, N. (2009). Computer aided engineering of an unmanned underwater vehicle, M.Sc. Thesis, Department of Mechanical Engineering, Middle East Technical University, Ankara.
- Costola, D. and Etheridge, D.W., (2008). Unsteady natural ventilation at model scale-Flow reversal and discharge coefficients of a short stack and an orifice. *Building and Environment*, 43:1491-1506.

- Çobanoğlu, İ. (2008). Experimental study of single and multiple outlets behavior under constant head, M.S. Thesis, Department of Civil Engineering, Middle East Technical University, Ankara.
- Dagan, Z., Sheldon, W. and Pfeffer, R. (1982). An infinite-series for the Creeping Motion through an Orifice of Finite Length, *J. of Fluid Mech.* 115: 505-523.
- Dally, J.W., Riley, W.F. and McConnell, K.G., (1993). *Instrumentation for engineering measurements*, USA: John Wiley & Sons.
- Daugherty, R.L. and Franzini, J.B., (1977). *Fluid Mechanics with Engineering Applications*. Mc Graw-Hill Book Company, USA; ISB 0-07-015427-9.
- Davis, C.V., (1952). *Handbook of applied hydraulics*, McGraw-Hill Book Company, Inc.
- Douglas, J.F., Gasiorek, J.M. and Swaffield, J.A., (2001). *Fluid Mechanics*. Prentice Hall; United Kingdom, ISBN 0 582 414768.
- Dziubinski, M. and Marcinkowski, A., (2006), Discharge of Newtonian and non-Newtonian liquids from tanks. *Chemical Engineering Research and Design*, 84(A12): 1194-1198.
- FLUENT 6.1. User's Manual to FLUENT 6.1. Fluent Inc., Centerra Resource Park, 10 Cavendish Court, Lebanon, USA, 2005.
- GAMBIT 2. User's Manual to GAMBIT 2. Fluent Inc., Centerra Resource Park, 10 Cavendish Court, Lebanon, USA, 2005.
- Gerges, H., and McCorquodale, J.A., (1997). Modelling of flow in Rectangular Sedimentation Tanks by Explicit Third-order Upwinding Technique, *Int. J. for Numerical Methods in fluids*, 24: 537-561.
- Göbelez, Ö., (2008). Experimental Analysis of the Flow through a Bottom Outlet on the Threshold of Motion of Particles. Msc Thesis. Middle East Technical University, Ankara.

- Gupta, R.S., (1989). Hydrology and Hydraulic Systems. Prentice Hall Inc., Englewood Cliffs, N.J.
- Hirt, C. W. and Nichols, B. D., (1981). Volume of Fluid (VOF) method for the dynamics of free boundaries, Journal of Computational Physics, Vol. 39: 201-225.
- Islam, M. R. and Zhu, D.Z., (2010). Flow Upstream of Two-Dimensional Intakes, J. of Hyd. Eng. doi:10.1061/(ASCE)HY. 1943-7900.0000284.
- Jankowski, T.A. Schmierer, E., Prenger, F.C. and Ashworth S.P., (2008). A series pressure drop representation for flow through Orifice tubes. J. of Fluids Engineering, ASME, 130: 051504-1-051504-7
- Judd, H. King, R.S., (1908). Some experiments on the frictionless orifice, Engr. News, 56(13), 326-330.
- Kiljanski, T., (1993). Discharge Coefficient for Free Jets from Orifices at Low Reynolds Number, J. of Fluids Engineering, ASME, 115:778-781.
- Lienhard (V), J.H. and Lienhard (IV), J.H., (1984). Velocity coefficients for free jets from sharp-edged orifices, Journal of Fluids Engineering, ASME, 106:13-17.
- Liu, S., Afacan, A. and Masliyah, J.H., (2001). A New Pressure Drop Model for Flow through Orifice Plates, Can. J. Chem.Eng.; 79:100-106.
- Medaugh, F.W., Johnson G.D., (1940). Investigation of the discharge coefficients of small circular orifices, Civil Engr., 7 (7):422-424.
- Merritt, H.E., (1967). Hydraulic Control Systems, Wiley & Sons.
- Munson, B.R., Young, D.F. and Okiishi, T.H., (1998). Fundamentals of Fluid Mechanics, Third edition, John Wiley & Sons, Inc., Canada. ISBN 0-471-17024-0.

- Patankar, S.V. (1980). Numerical Heat Transfer and Fluid Flow. Mc Graw-Hill Company, New York.
- Peker, E.A. (2005). Momentum exchange in coaxial change flows. M.Sc. Thesis, Department of Civil Engineering, Middle East Technical University, Ankara
- Phares, D.J., Smedley, G.T. and Zhou J., (2005). Laminar Flow Resistance in Short Microtubes. *Int. J. Heat Fluid Flow*; 26: 506–512.
- Ramamurthi, K. and Namdakumar, K., (1999). Characteristics of flow through small sharp-edged cylindrical orifices. *Flow Measurement and Instrumentation*; (10): 133-143.
- Rhie, C.M. and Chow, W.L., (1983). Numerical study of the turbulent flow past an airfoil with trailing edge separation. *AIAA Journal*, 21:1525–1532
- Shammaa, Y., Zhu, D. Z. and Rajaratnam, N., (2005). Flow upstream of orifices and sluice gates. *Journal of Hydraulic Engineering*, 131(2), 127-133.
- Shammaa, Y. and Zhu, D.Z. (2010). Experimental study on selective withdrawal in a two-layer reservoir using a temperature-control curtain. *ASCE Journal of Hydraulic Engineering*, 136(4), 234-246.
- Swamee, P.K. and Swamee, N., (2010). Discharge Equation of Circular Sharp-Crested Orifice, *Journal of Hydraulic Research*, 48 (1): 106-107.
- Simon, A.L., (1981), *Practical Hydraulics*, Second Edition. John Wiley and Sons, USA. ISBN -471-05381-3.
- Streeter, V.L., (1966). *Fluid Mechanics*, McGraw-hill Book Company, Japan.
- Tığrek, Ş. (1990). Pressure Drop Due to Entrance Region for a Turbulent Flow in Closed Conduit. Middle East Technical University, Ankara.

- Tu, X., Hrnjak, P.S. and Bullard C.W., (2006). Refrigerant 134a Liquid Flow through Micro-Scale Short Tube orifices With/Without Phase Change. *Exp. Therm. Fluid Sci.*, 30: 253-262.
- Yang, L. and Zhang, C.L., (2005). Two-fluid model refrigerant two-phase flow through slot orifice, *International Journal of Refrigeration*, 28: 419-427.
- Youngs, D.L., (1982). Time-dependent multi-material flow with large fluid distortion. In: K.W. Morton and M.J. Baines, Editors, *Numerical Methods for Fluid Dynamics*, Academic Press (1982).